IMPROVE REPORT V

OVERVIEW AND SUMMARY

S.1 INTRODUCTION

This report describes aerosol speciation data collected by the Interagency Monitoring of Protected Visual Environments (IMPROVE) network. The IMPROVE program is a cooperative measurement effort between the U. S. Environmental Protection Agency (EPA), federal land management agencies, and state agencies. The network is designed to

1. establish current visibility and aerosol conditions in 156 mandatory Class I areas (CIAs);
2. identify chemical species and emission sources responsible for existing anthropogenic visibility impairment;
3. document long-term trends for assessing progress towards the national visibility goal;
4. and, with the enactment of the Regional Haze Rule, provide regional haze monitoring representing all visibility-protected federal CIAs where practical.

This report is the fifth in a series of IMPROVE reports that describes the monitoring methods and changes to instrumentation over time, as well as reports on measured aerosol concentrations and aerosol-derived visibility estimates. This report does not include data summaries of IMPROVE's direct atmospheric optical monitoring using nephelometers and transmissometers and scene monitoring using still and video camera systems. The IMPROVE and FED[1] web sites include descriptions of the aerosol, optical, and scene monitoring activities and provide access to the resulting data.

Air quality measurements in the IMPROVE network began in 1988. Due to resource and funding limitations in the early network, measurements in all 156 mandatory Class I areas were not possible. Instead, 36 sites were selected to represent aerosol concentrations and visibility over the United States. The first IMPROVE report was published in 1993 and described data that were collected at the initial 36 sites from March 1988 through February 1991 (Sisler et al., 1993). Beginning with the initial report, and in the reports that followed, spatial patterns and seasonal trends in speciated aerosol concentrations and reconstructed light extinction coefficients were presented. In addition, in the first report, focus was placed on aerosol measurement quality, aerosol acidity, and transmissometer measurements. In 1996 the second IMPROVE report was published and described data from March 1992 through February 1995 from 43 sites in the network (Sisler et al., 1996). In addition to spatial and seasonal trends, the second report included an exploration of aerosol light extinction efficiencies and long-term trends in fine mass and sulfur, using stacked filter unit measurements. In 2000, the third IMPROVE report was produced that included descriptions of data from 49 sites during the period from March 1996 through February 1999 (Malm et al., 2000). In addition to spatial and seasonal trends, this report included a discussion of the contributions of aerosol species to periods of high and low mass concentrations. Temporal (long-term and diurnal) trends in visibility and aerosol concentration were also reported. The fourth report was published in 2006 and covered data from 2000 through 2004 (Debell et al., 2006). The number of sites increased to 159 due to the expansion of the

[1] The VIEWS website, where data were previously available, has recently transitioned to the Federal Environmental Database (FED) website (http://views.cira.colostate.edu/fed/).

network to meet the goals of the Regional Haze Rule. In addition to data from the IMPROVE sites, data from 84 sites from the EPA's Speciated Trends Network (STN) were included to expand the spatial and seasonal aerosol and reconstructed light extinction coefficient trends to include urban areas and to investigate the differences in urban and rural aerosol concentrations. The 2006 report also included an initial investigation into the comparability of IMPROVE and STN data. Focus was also placed on IMPROVE quality assurance procedures.

At the timing of this report, the IMPROVE network consisted of 212 sites (170 current and 42 discontinued sites). This report, the fifth in the series, describes analyses for the 2005–2008 time period for 168 IMPROVE sites and 176 sites from the EPA's Chemical Speciation Network (CSN, formally STN). As in the previous reports, the fifth report includes the spatial and seasonal trends in aerosol mass and reconstructed light extinction coefficients for major aerosol species, including sea salt for the first time. The additional analyses in this report include an examination of urban and rural aerosol differences ("urban excess") and their spatial patterns using IMPROVE and CSN data. A deeper exploration of the seasonality in speciated aerosol mass concentrations and reconstructed light extinction coefficients is also presented. With the long temporal record of IMPROVE data, "long-term" (1989–2008) and "short-term" (2000–2008) trends in speciated aerosol concentrations for seasonal and statistical parameters were explored. Descriptions of regional haze metrics, including comparisons of visibility between the Regional Haze Rule baseline period (2000–2004) and period 1 (2005–2009) are presented. An assessment of biases in fine mass measurements is also included. The following summary provides highlights of the material contained in the fifth (2011) IMPROVE report; the reader is encouraged to refer to the full report for more detail.

S.2 AEROSOL DATA

The version II IMPROVE sampler, deployed in 2000, consists of four independent modules (A, B, C, and D) that collect 24-hour samples every third day. Each module incorporates a separate inlet, filter pack, and pump assembly. Modules A, B, and C are equipped with a 2.5 µm cyclone that allows for sampling of particles with aerodynamic diameters less than 2.5 µm, while module D is fitted with a PM_{10} inlet to collect particles with aerodynamic diameters less than 10 µm. Each module contains a filter substrate specific to the analysis planned. Module A is equipped with at Teflon® filter that is analyzed for $PM_{2.5}$ gravimetric fine mass, elemental concentration, and light absorption. Module B is fitted with a Nylasorb (nylon) filter and analyzed for the anions sulfate, nitrate, nitrite, and chloride using ion chromatography. Module C utilizes a quartz fiber filter that are analyzed by thermal optical reflectance (TOR) for organic and light absorbing carbon (OC and LAC, respectively) (Chow et al., 1993). We use the term "light absorbing carbon" instead of "elemental carbon" or "EC" in this report to reflect the recent literature regarding light absorption by carbonaceous aerosols (Bond and Bergstrom, 2006). Finally, module D is fitted with a PM_{10} inlet and utilizes a Teflon filter. PM_{10} aerosol mass concentrations are determined gravimetrically. Details regarding aerosol sampling and analyses can be found in Chapter 1. IMPROVE data are available for download from http://views.cira.colostate.edu/fed/. Current and discontinued IMPROVE sites are listed by region in Table 1.1 in Chapter 1. A map of IMPROVE sites (grouped by region) is shown in Figure S.2.1. See Chapter 1 for more detail regarding how the regions were specified.

CSN data were also used extensively in this report. CSN operates approximately 50 long-term-trend sites, with another ~150 sites operated by state, local, and tribal agencies, primarily in urban/suburban settings. All CSN samplers utilize a $PM_{2.5}$ inlet and three channels containing Teflon, nylon, and quartz filters. Like the IMPROVE network, CSN samplers operate on a 24-hour schedule from midnight to midnight every third day. $PM_{2.5}$ gravimetric mass and elemental compositions are analyzed from the Teflon filter, ions from the nylon filter, and carbon from the quartz filter. The carbon analysis was historically performed with thermal optical transmittance (TOT) using a NIOSH-type protocol. The recognition that IMPROVE samplers and TOR analysis produce different OC and LAC concentrations than CSN samplers and TOT analysis has motivated the CSN transition to TOR analysis for consistency with the IMPROVE network. In addition to the transition from TOT to TOR, in April 2005 EPA decided to replace the carbon channel sampling and analysis methods with a URG 3000N sampler that is similar to the IMPROVE version II module C sampler. The conversion began in May 2007 with 56 sites, followed by another 63 sites in April 2009 and 78 additional sites in October 2009. Additional detail regarding IMPROVE and CSN sampling and analysis methods for each species is provided in Chapter 2 and includes a discussion of aerosol species mass calculations. A discussion of the adjustments developed for this report and applied to CSN carbon data collected prior to the transition to the new analyses and monitors is also included. Adjustments to CSN carbon data were required for IMPROVE and CSN data to be combined. A map of 321 CSN sites is provided in Figure S.2.2 with the general regions depicted. A subset of these sites (176) was used in this report, based on completeness criteria outlined in Chapter 2. A description of the how the regions were defined is in Chapter 1.4.

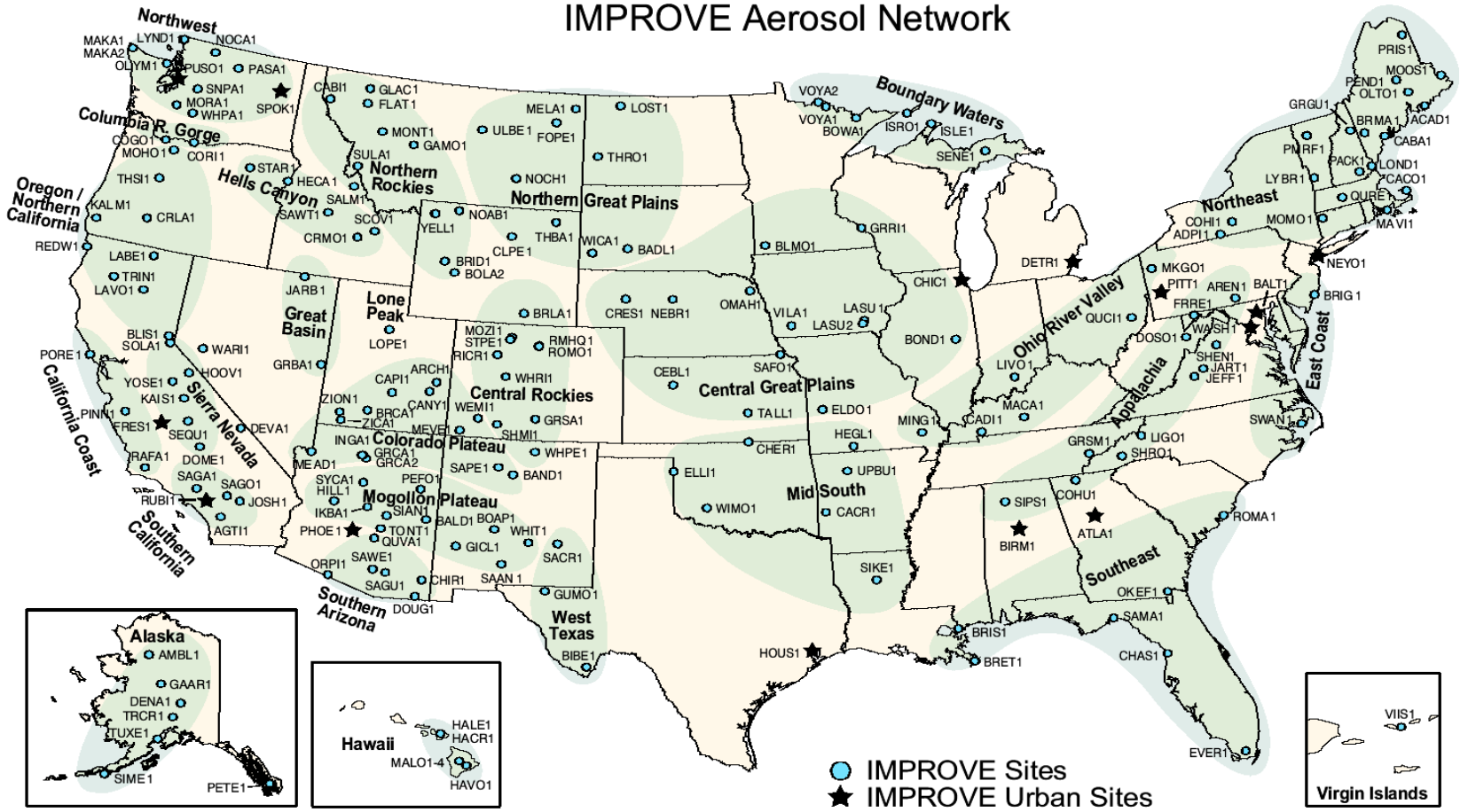

Figure S.2.1. Locations of IMPROVE and IMPROVE protocol sites for all discontinued and current sites. The IMPROVE regions used for grouping the sites are indicated by shading and bold text. Urban sites included in the IMPROVE network for quality assurance purposes are identified by stars.

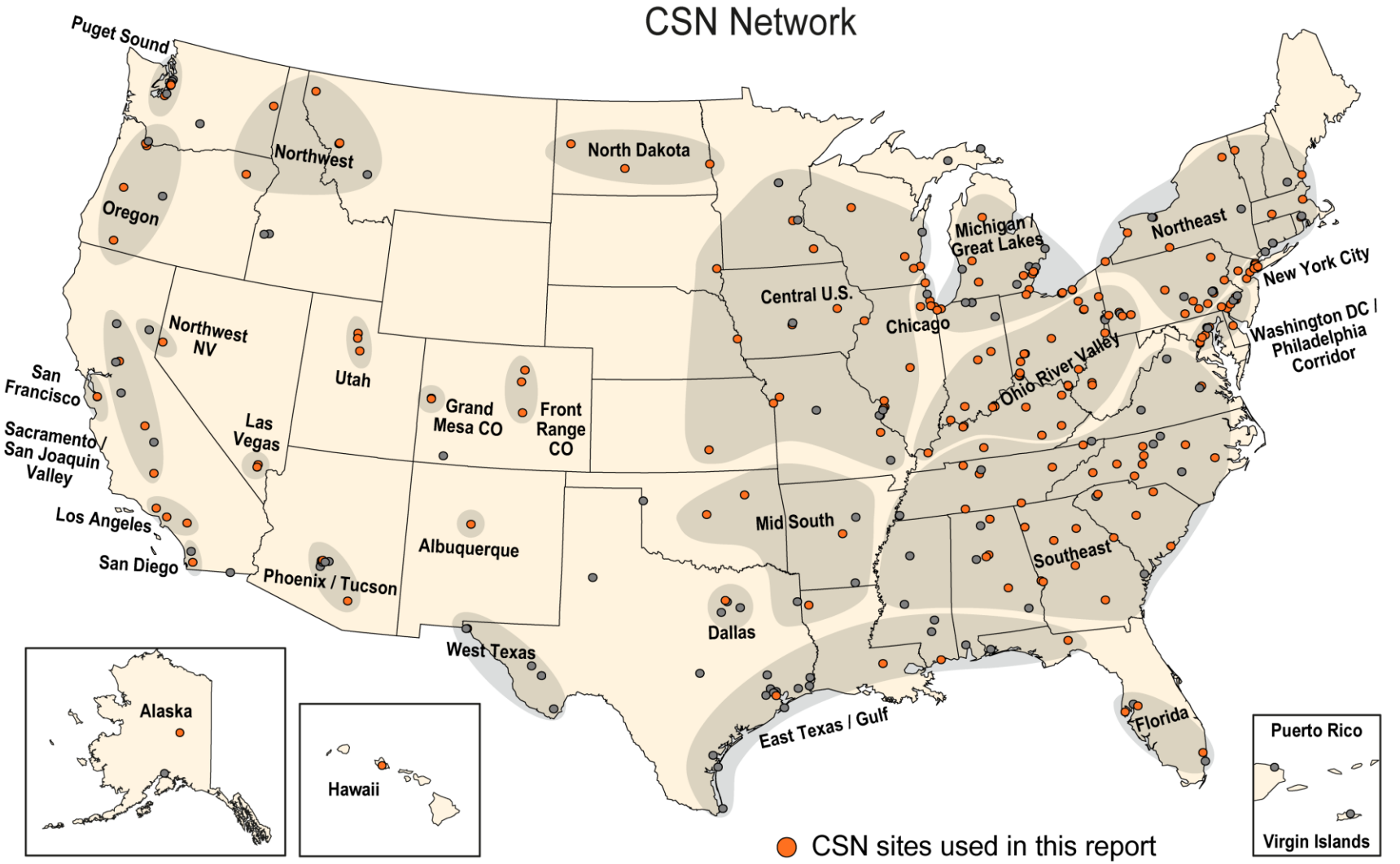

Figure S.2.2. Current and discontinued Chemical Speciation Network (CSN) sites (grey and orange) operated by the Environmental Protection Agency. Regions are shown as shaded areas and bold text. The sites included in the analyses in this report are shown as orange circles.

The IMPROVE and CSN networks operate collocated samplers in several urban sites. Collocated sites with data that met the completeness criteria outlined in Chapter 2 were compared to identify relative biases between IMPROVE and CSN speciated aerosol concentrations. Daily data from Baltimore, Maryland; Birmingham, Alabama; Fresno, California; New York City (Bronx), New York; Phoenix, Arizona; Puget Sound (Seattle), Washington; and Washington, D.C. for 2005–2008 were used. Ammonium sulfate (AS), ammonium nitrate (AN), organic carbon (OC), light absorbing carbon (LAC), soil, sea salt, $PM_{2.5}$ gravimetric fine mass (FM), and reconstructed fine mass (RCFM) were compared. A summary of results is provided in Table S.2.2. Errors were fairly low for most species (<20%), with the exception of soil (37.0%) and sea salt (78.3%), which also had high biases. IMPROVE sea salt concentrations were computed as 1.8 times chloride ion concentrations, whereas CSN sea salt concentrations were computed as 1.8 times chlorine concentrations. However, biases for other species were generally low, ranging from 5.7% for LAC to 18.4% for FM. The errors and relative biases between unadjusted CSN carbon and IMPROVE carbon data were 95.9% and 111.2 % for OC, respectively, and 26.7% and -17.3% for unadjusted LAC, respectively. The close agreement in adjusted OC and LAC data suggests that the adjustments applied to those data were appropriate and effective (see Chapter 2). It should also be noted that while IMPROVE applies artifact corrections to ion data, CSN does not; some of the discrepancy between ion data from the two networks could be due this difference.

The large errors and biases for soil and sea salt indicate that IMPROVE had much higher concentrations compared to CSN concentrations. Recall that these data are from collocated sites so the biases reflected differences in sampling or analytical techniques. The biases in soil and sea salt are sufficiently large that combined data analyses should be treated as semiquantitative. CSN concentrations were somewhat higher than IMPROVE concentrations for most other species (positive biases correspond to higher CSN concentrations), but data from the two networks were fairly highly correlated. The general agreement for most species indicates that it was appropriate to combine data.

Table S.2.2. Comparisons between collocated IMPROVE and CSN sites for all data from 2005 through 2008. Species include organic carbon (OC), light absorbing carbon (LAC), ammonium sulfate (AS), ammonium nitrate (AN), soil, sea salt, $PM_{2.5}$ gravimetric fine mass (FM), and $PM_{2.5}$ reconstructed fine mass (RCFM). "OC_{unadj}" and "LAC_{unadj}" refer to comparisons between unadjusted CSN carbon data and IMPROVE carbon data; "OC_{adj}" and "LAC_{adj}" refer tocomparisons between adjusted CSN carbon and IMPROVE carbon data.

Statistic	OC_{unadj}	LAC_{unadj}	OC_{adj}	LAC_{adj}	AS[3]	AN[4]	Soil	Sea salt[5]	FM	RCFM
Average IMPROVE ($\mu g\ m^{-3}$)	2.8	1.3	2.7	1.2	3.9	2.3	1.4	0.3	12.6	13.5
Average CSN ($\mu g\ m^{-3}$)	5.2	1.0	3.0	1.2	4.1	2.6	0.9	0.11	14.3	13.5
Bias[1] (%)	111.2	-17.3	8.3	5.7	7.0	17.2	-31.0	-62.8	18.4	0.04
Error[2] (%)	95.9	26.7	16.0	20.2	7.5	13.9	37.0	78.3	14.1	8.5
r	0.92	0.87	0.93	0.88	0.98	0.99	0.85	0.84	0.9	0.95
IMP/CSN	0.54	1.3	0.93	1.0	0.96	0.92	1.6	3.2	0.9	1.0
Number of data points (N)	2087	2077	2675	2665	2687	2689	2646	1904	2636	2535

[1] $\text{Error} = \text{median}\left(\left|\frac{\overline{X}_i - \overline{Y}_i}{\overline{Y}_i}\right|\right)$

[2] $\text{Bias} = \frac{1}{N}\sum_i^N \frac{\overline{X}_i - \overline{Y}_i}{\overline{Y}_i}$; $\overline{X}_i$ and $\overline{Y}_i$ are the daily data for CSN and IMPROVE concentrations, respectively. The number of data points is given by N.

[3] AS = 1.375[sulfate ion]

[4] AN = 1.29[nitrate ion]

[5] Sea salt = 1.8[chloride ion] for IMPROVE and 1.8[chlorine] for CSN.

S.3 SPATIAL PATTERNS IN RURAL AND URBAN SPECIATED AEROSOL CONCENTRATIONS: IMPLICATIONS FOR URBAN EXCESS

Urban excess is defined as the difference in aerosol mass concentrations at an urban site compared to the regional background concentration. Urban excess studies provide estimates of the relative magnitude of local versus regional contributions to aerosol concentrations and subsequently increase our understanding of aerosol sources and lifetimes in the atmosphere. Different aerosol species correspond to a range in urban excess values, depending on their sources and lifetimes.

Data from 344 IMPROVE and CSN sites were combined to explore the spatial variability in major aerosol species, as well as their impacts on urban excess. Urban excess was investigated for 2005–2008 annual mean ammonium sulfate (AS), ammonium nitrate (AN), particulate organic matter (POM=1.8OC), light absorbing carbon (LAC), and $PM_{2.5}$ gravimetric fine mass (FM). Sea salt and fine soil were not included because of the relative biases derived for those species from analyses of data from collocated IMPROVE and CSN sites (see Table S.2.2), nor was coarse mass as CSN does not monitor for it. Although urban excess estimates were computed for annual mean concentrations, estimates undoubtedly varied temporally, as the seasonal aerosol concentrations for urban and rural sources were very distinct (see section S.4 and Chapter 4 in the main report). Urban excess estimates, defined as the ratio of urban to rural

concentrations, for AS, AN, POM, and LAC are summarized here; further discussions regarding the spatial variability and urban excess in mass concentrations, including the absolute differences in concentration, in these and other species can be found in Chapter 4 and Chapter 7, respectively.

Isopleth maps of annual mean mass concentrations were created for each species for combined IMPROVE and CSN data. Isopleth maps created using a Kriging algorithm should be viewed and interpreted with caution. The isopleths are intended to help visualize the data and identify large spatial patterns only. Similar maps were created for urban excess estimates.

Regional background concentrations at urban locations were determined from interpolated rural IMPROVE data at the grid cell corresponding to a CSN urban site. Urban sites were limited to locations with at least one IMPROVE site within 150 km, resulting in 114 CSN sites used in the urban excess analysis. Urban CSN data (not interpolated data) were used. No elevation corrections (standard pressure and temperature) were applied to the urban and rural data, with the assumption that if the sites were within 150 km, the corrections based on elevation differences would be negligible (it is unlikely that a site at sea level would be 150 km from a site at an elevation of 3 km). A more important elevation issue is the possibility that urban and rural sites with a significant elevation difference were actually sampling different air masses as some IMPROVE monitors could be above the boundary layer (e.g., Rocky Mountain National Park and Denver, Colorado).

S.3.1 Ammonium Sulfate

The spatial distribution of AS with the rural and urban sites combined (see Figure S.3.1a) was very similar to the pattern of the rural sites alone (see Chapter 2), suggesting that regional impacts of high AS concentrations influenced both urban and rural sites similarly. Notice the difference in site density between the IMPROVE and CSN networks in Figure S.3.1.a, with many more CSN sites in the eastern United States; these sites provide additional detail to the spatial patterns of AS in that section of the country. The combination of high sulfur dioxide emissions and high relative humidity produced the highest concentrations (4–8 $\mu g\ m^{-3}$) of AS in the eastern United States that centered on the Ohio River valley and Appalachia regions. AS concentrations decreased sharply towards the western United States. In fact, concentrations in the western United States were typically less than 2 $\mu g\ m^{-3}$.

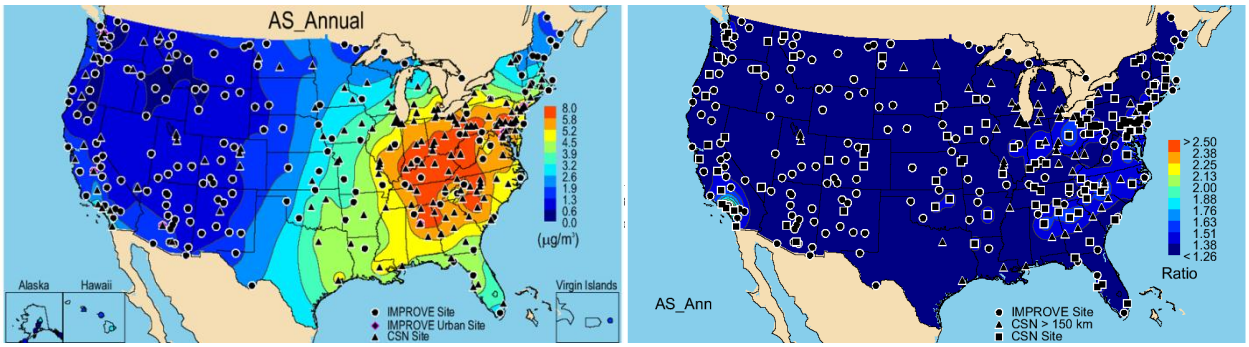

Figure S.3.1. (a) IMPROVE and CSN $PM_{2.5}$ ammonium sulfate (AS) 2005–2008 annual mean mass concentrations (μg m^{-3}). (b) Interpolated ratios of urban (CSN) to rural (IMPROVE) annual mean AS concentrations for 2005–2008. IMPROVE sites are shown as circles; CSN sites used in the analysis are shown as squares. CSN sites with no IMPROVE site within 150 km are shown as triangles. These sites were not used in the analysis.

The ratio of urban to rural AS concentrations is shown in Figure S.3.1b. CSN site locations with an IMPROVE monitor within 150 km are depicted with square symbols; sites not meeting this criteria are shown as triangles. In addition to the southern California area, higher ratios occurred for a swath of area southeast of the Appalachia Mountains and the Ohio River valley. The lowest ratios occurred in the central, western, northwestern, and northeastern United States. Similar concentrations of AS for rural and urban sites suggested strong regional impacts, not surprising given the regional nature of its sources; however, some urban excess in AS occurred. The mean (one standard deviation) ratio for all 114 urban sites was 1.4 ± 0.3. Some of the excess could be explained by the small relative bias between AS data from the CSN and IMPROVE networks (Table S.2.2).

S.3.2 Ammonium Nitrate

Not surprisingly, locations where ammonia and nitric acid concentrations were the highest corresponded to the regions where AN concentrations were the largest (Figure S.3.2a). Higher sources of precursors to AN in agricultural regions in the Midwest resulted in the highest AN concentrations for rural sites in the United States. Generally, urban concentrations of AN were considerably higher than rural concentrations. Urban concentrations were also higher in the Midwest and were considerably higher than rural concentrations in the same region.

The impacts of urban sources of AN to surrounding rural regions were apparent by examining the ratio of urban to rural AN concentrations as shown in Figure S.3.2b. Several western cities corresponded to relatively high ratios with sharp spatial gradients. Significant urban excess was expected in the Midwest based on the differences in the rural and urban concentrations in that region. However, none of the urban sites in that area were associated with rural sites within 150 km; therefore low urban excess in that area was due to lack of data. The mean ratio (one standard deviation) was 2.5±1.3, considerably higher than the mean ratio for AS. Relative biases in AN data from the IMPROVE and CSN networks contributed slightly.

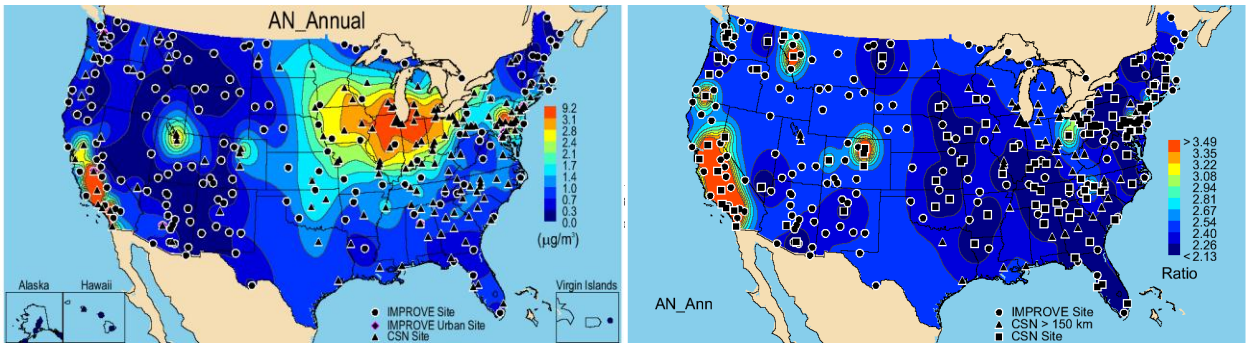

Figure S.3.2. (a) IMPROVE and CSN $PM_{2.5}$ ammonium nitrate (AN) 2005–2008 annual mean mass concentrations (μg m^{-3}). (b) Interpolated ratios of urban (CSN) to rural (IMPROVE) annual mean AN concentrations for 2005–2008. IMPROVE sites are shown as circles; CSN sites used in the analysis are shown as squares. CSN sites with no IMPROVE site within 150 km are shown as triangles. These sites were not used in the analysis.

S.3.3 Particulate Organic Matter

The highest rural annual mean POM concentrations corresponded to a large area in the southeastern United States (Figure S.3.3a), most likely associated with biogenic emissions and perhaps biomass smoke emissions (Tanner et al., 2004; Bench et al., 2007). The western United States was associated with more localized regions of higher POM concentrations; rural concentrations in Idaho and Montana were near 3 μg m^{-3}, most likely from biomass burning emissions. Higher POM concentrations and more localized impacts of urban POM sources were apparent in the western United States, with sharper gradients compared to the eastern United States.

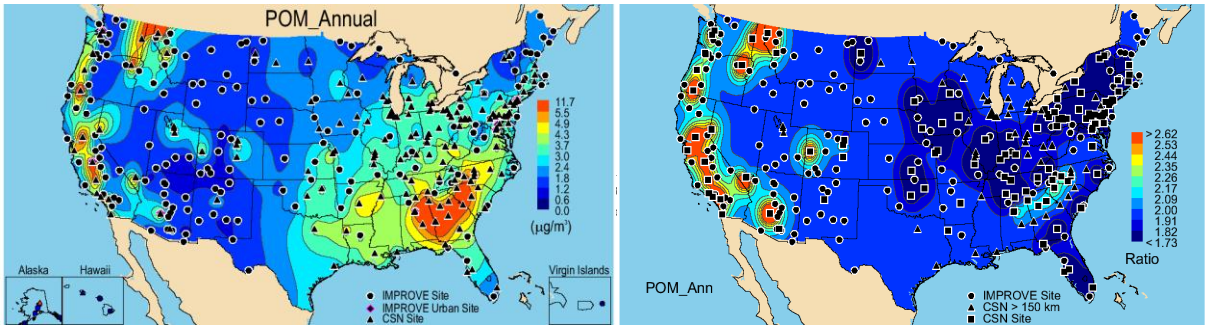

Figure S.3.3. (a) IMPROVE and CSN $PM_{2.5}$ particulate organic matter (POM) 2005–2008 annual mean mass concentrations (μg m^{-3}). (b) Interpolated ratios of urban (CSN) to rural (IMPROVE) annual mean POM concentrations for 2005–2008. IMPROVE sites are shown as circles; CSN sites used in the analysis are shown as squares. CSN sites with no IMPROVE site within 150 km are shown as triangles. These sites were not used in the analysis.

Urban excess estimates for POM did not account for different types of organic aerosols known to exist in urban versus rural settings. Urban organic aerosols from local sources are less aged and correspond to lower molecular weight per carbon weight ratios compared to rural aerosols (e.g., Turpin and Lim, 2001). The difference in the organic carbon multiplier for urban versus rural aerosols was not accounted for in this analysis (a value of 1.8 was applied to both), although Malm et al. (2011) suggested that the urban organic multiplier was 5–15% lower than

that for rural sites after investigating biases in fine mass data from the IMPROVE and CSN networks.

The pattern of localized influences seen in Figure S.3.3a is displayed more clearly as the urban to rural POM concentration ratio in Figure S.3.3b. Several western cities were associated with higher ratios (urban concentrations over 2.5 times higher than rural concentrations). Ratios of ~2.3 corresponded to a swath of area to the southeast of the Appalachia Mountains the eastern United States. This area was associated with the highest urban concentrations and the fewest number of IMPROVE sites. Urban concentrations were 1.9 ± 0.9 times higher than rural concentrations on average, although relative biases between data from the two networks contributed slightly to this excess. The mean POM ratio was higher than the mean AS ratio, but lower than the AN ratio, suggesting that POM was more regional in extent in some areas of the country (e.g., southeastern United States) but also was influenced by local urban sources.

S.3.4 Light Absorbing Carbon

The IMPROVE rural annual mean LAC concentrations in the western United States typically were less than ~0.3 μg m^{-3}. The rural concentrations in the eastern United States were higher (0.4–0.5 μg m^{-3}) and tended to be located in the southern United States and Ohio River valley areas, as well as parts of Pennsylvania (Figure S.3.4a). Major hotspots of LAC concentrations were associated with urban sites. Urban LAC concentrations generally were localized around individual site locations in the western United States and were more regional in extent in the eastern United States, although not to the degree of POM. The largest urban LAC concentrations were near 2.5 μg m^{-3}.

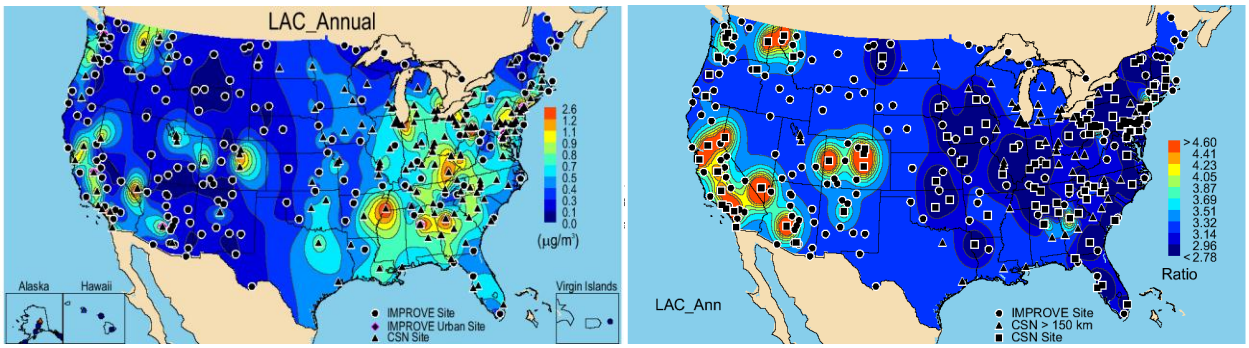

Figure S.3.4. (a) IMPROVE and CSN $PM_{2.5}$ light absorbing carbon (LAC) 2005–2008 annual mean mass concentrations (μg m^{-3}). (b) Interpolated ratios of urban (CSN) to rural (IMPROVE) annual mean LAC concentrations for 2005–2008. IMPROVE sites are shown as circles; CSN sites used in the analysis are shown as squares. CSN sites with no IMPROVE site within 150 km are shown as triangles. These sites were not used in the analysis.

The ratio of urban to rural LAC concentrations demonstrated the localized impact from primary emissions of LAC on surrounding rural regions. Fewer sites in the eastern United States were associated with higher ratios compared to western sites (Figure S.3.4b). Although areas associated with high ratios were similar for POM and LAC, LAC ratios were much larger, suggesting urban LAC sources were significantly larger than rural sources. In addition, LAC urban excess estimates were less regional in extent than POM, indicating local source contributions of LAC rather than more regional sources like biomass combustion from controlled

or wild fires. The mean ratio was 3.3 ± 1.9 and was much larger than the mean ratio for AS, AN, or POM.

Analyses of interpolated IMPROVE and CSN aerosol concentrations provided spatial patterns of urban excess for the United States. For certain species, such as POM, LAC, and AN, annual mean urban concentrations were considerably higher than rural concentrations. As a summary, the urban excess mean ratios for AS, AN, POM, and LAC were 1.4 ± 0.3, 2.5 ± 1.3, 1.9 ± 0.9, and 3.3 ± 1.9, respectively. Although not shown here, the mean FM ratio was 2.0 ± 0.6. Urban excess values include the relative biases between data from the two networks. Urban excess estimates varied widely as a function of location. While the isopleths of urban excess were semiquantitative, they indicated the spatial extent of urban impacts on surrounding rural and remote areas as a function of species. For example, while LAC corresponded to the highest mean urban to rural concentration ratio, its spatial extent was generally the lowest and associated with sharp spatial gradients, suggesting local sources. In contrast, the spatial patterns in urban excess associated with species such as AS, POM, and FM were more regional in extent, especially in the eastern United States, although impacts from local sources were also apparent.

S.4 SEASONAL DISTRIBUTIONS IN AEROSOL MASS CONCENTRATIONS

The seasonality of speciated aerosol mass concentrations can be significant depending on species and region and is a function of the source emissions, meteorological parameters, and local and long-range transport. Examining aerosol concentrations on a regional basis, rather than a site-specific basis, can lead to insights regarding air quality issues on regional scales.

IMPROVE and CSN data from 2005 through 2008 were regionally and monthly averaged according to previously defined regions (see Section S.2 and Chapter 1.2 and 1.4) and plotted as stacked bar charts on maps of the United States. The CSN and IMPROVE regions coincide a closely as possible, but do depend on available sites in a given area. Some regions consist of only one site (e.g., IMPROVE urban sites). The monthly mean concentrations of ammonium sulfate (AS), ammonium nitrate (AN), particulate organic matter (POM), light absorbing carbon (LAC), soil, sea salt, and gravimetric fine mass (FM) and coarse mass (CM) were computed. Stacked bar charts provide a detailed view of the changes in monthly mean aerosol concentrations during the year at different regions in the United States. In addition, analyses were performed that complement the stacked bar charts by summarizing the detailed information in the bar charts in such a way that quickly and easily convey the temporal changes in the data. Seasonality was defined in terms of the ratio of the maximum to minimum monthly concentration for a given region. Seasonal periods included winter (December, January, and February), spring (March, April, and May), summer (June, July, and August), and fall (September, October, and November). Maps of seasonality were created in which each region was associated with a set of triangles. The color of the upward-pointing triangle refers to the season with the maximum monthly mean concentration. The color of the downward-pointing triangle refers to the season with the minimum monthly mean concentration. The size of the triangle corresponds to the ratio of maximum to minimum monthly concentration such that large triangles represent larger degrees of seasonality. The location of the triangle on the map represents the region and may not be placed directly over a specific site location. Highlights in seasonality of mass concentrations for IMPROVE and CSN concentrations are included here; additional detail, including regional

stacked bar charts, are provided in Chapter 4. Similar results for reconstructed light extinction coefficients are reported in Chapter 5.

S.4.1 Ammonium Sulfate

AS was associated with a high degree of seasonality, with the majority of IMPROVE regions corresponding to ratios of maximum to minimum monthly mean mass concentrations greater than 2 (Figure S.4.1a). The maximum AS mass concentrations were predominantly observed in summer at many IMPROVE regions, with the exception of spring maxima in the northwestern United States. The minimum season for almost all regions occurred in winter. AS concentrations at CSN regions were somewhat less seasonal than rural regions (Figure S.4.1b). Most CSN regions corresponded to summer maxima and winter and fall minima.

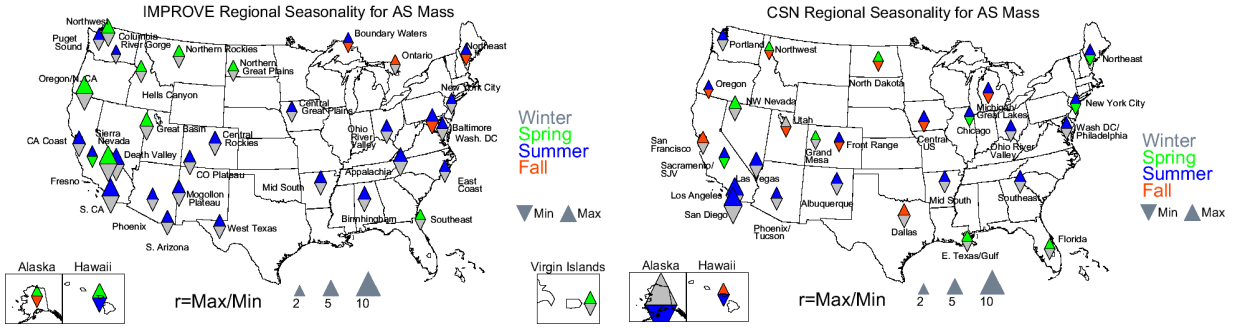

Figure S.4.1. (a) Seasonal variability for 2005–2008 monthly mean IMPROVE ammonium sulfate (AS) mass concentrations. (b) The same as (a), but for the CSN. The color of the upward-pointing triangle refers to the season with the maximum monthly mean concentration, and the downward-pointing triangle refers to the season with the minimum monthly mean concentration. The size of the triangles refers to the magnitude of the ratio of maximum to minimum monthly mean mass concentration.

S.4.2 Ammonium Nitrate

IMPROVE rural AN concentrations were typically higher in winter due to more favorable conditions of nitrate particle formation in that season. The winter maxima at most regions were very obvious from the depiction of seasonality in Figure S.4.2a. Most of the IMPROVE regions were associated with a high degree of seasonality in monthly mean AN concentrations. CSN regions demonstrated a strong seasonality, with only one region having a maximum to minimum ratio less than or equal to 2 (Florida, 2.0) (Figure S.4.2b). The maximum monthly mean AN concentration occurred in winter for the majority of CSN regions. More urban regions corresponded to winter maxima compared to the IMPROVE regions and were subject to a higher degree of seasonality. Western regions had higher seasonality than eastern regions. Many regions had minimum concentrations in the fall.

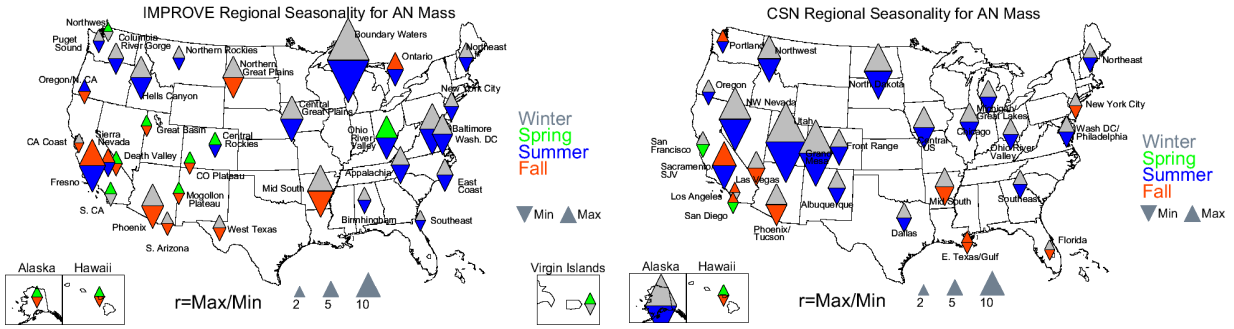

Figure S.4.2. (a) Seasonal variability for 2005–2008 monthly mean IMPROVE ammonium nitrate (AN) mass concentrations. (b) The same as (a), but for the CSN. The color of the upward-pointing triangle refers to the season with the maximum monthly mean concentration, and the downward-pointing triangle refers to the season with the minimum monthly mean concentration. The size of the triangles refers to the magnitude of the ratio of maximum to minimum monthly mean mass concentration.

S.4.3 Particulate Organic Matter

Most of the IMPROVE regions demonstrated a high level of seasonality in monthly mean POM concentrations (Figure S.4.3a). The western United States corresponded to much higher seasonality in IMPROVE POM concentrations compared to the eastern United States, probably because of the impacts from biomass burning in summer. Most western regions had summer maxima and winter minima, with the exception of the IMPROVE urban sites of Fresno, Phoenix, and Puget Sound, all of which had winter maxima. A few regions had spring minima. In the eastern United States, the maxima predominantly occurred in summer, but minima occurred during all seasons. Maximum and minimum can both occur in the same season (i.e., Baltimore). The seasonality of POM monthly mean concentrations was much different for urban CSN regions compared to rural IMPROVE regions. Lower seasonality was observed in general, and the winter minima/summer maxima that occurred in most western IMPROVE regions (and Alaska) were replaced with nearly the opposite: winter maxima and spring and summer minima (Figure S.4.3b). In the eastern United States, the seasonality varied per region, with several regions having summer maxima and winter and spring minima. Several regions along the eastern coast corresponded to similar summer maxima/spring minima and degree of seasonality as the rural regions.

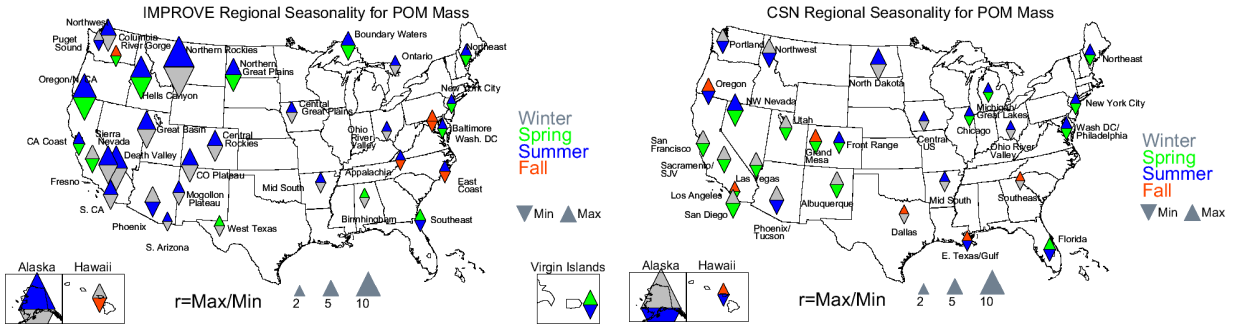

Figure S.4.3. (a) Seasonal variability for 2005–2008 monthly mean IMPROVE particulate organic matter (POM) mass concentrations. (b) The same as (a), but for the CSN. The color of the upward-pointing triangle refers to the season with the maximum monthly mean concentration, and the downward-pointing triangle refers to the season with the minimum monthly mean concentration. The size of the triangles refers to the magnitude of the ratio of maximum to minimum monthly mean mass concentration.

S.4.4 Light Absorbing Carbon

IMPROVE LAC monthly mean concentrations corresponded to some degree of seasonality, although less than POM concentrations. Western regions corresponded to a higher degree of seasonality compared to the eastern United States (Figure S.4.4a). Many western regions corresponded to summer maxima and winter minima. Similar to POM concentrations, some of the urban IMPROVE regions had the opposite seasonality (winter maxima/summer minima). Several eastern regions corresponded to fall maxima. CSN LAC concentrations demonstrated a degree of seasonality similar to urban POM concentrations, but with different seasons corresponding to maximum and minimum, especially in the eastern United States (Figure S.4.4.b). Several western regions corresponded to winter maxima and spring minima and higher seasonality compared to eastern regions. In contrast, several eastern regions had fall maxima and summer minima.

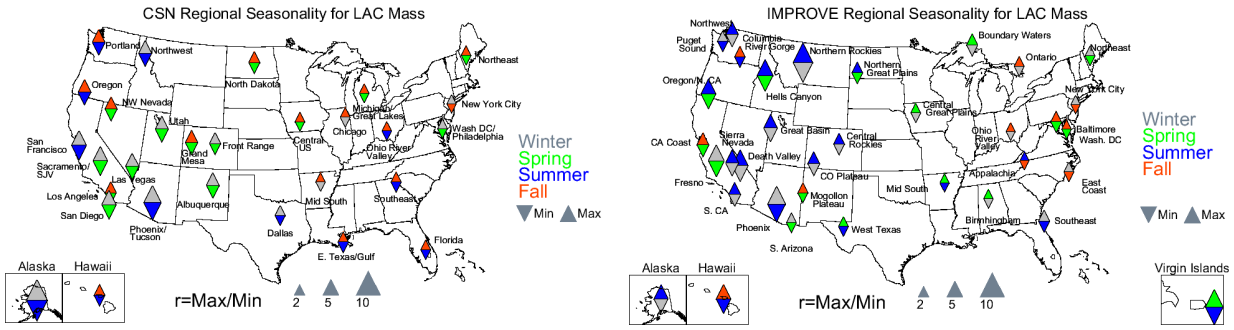

Figure S.4.4. (a) Seasonal variability for 2005–2008 monthly mean IMPROVE light absorbing carbon (LAC) mass concentrations. (b) The same as (a), but for the CSN. The color of the upward-pointing triangle refers to the season with the maximum monthly mean concentration, and the downward-pointing triangle refers to the season with the minimum monthly mean concentration. The size of the triangles refers to the magnitude of the ratio of maximum to minimum monthly mean mass concentration.

S.4.5 $PM_{2.5}$ Soil Mass

IMPROVE monthly mean soil concentrations were highly seasonal, with only four regions having maximum to minimum ratios less than 2 (all urban regions), consistent with the often episodic impacts of soil emissions. Maxima occurred primarily in the spring in the western and southwestern United States and in summer in the northwestern and eastern United States for most regions, and minima often occurred in winter. CSN urban regions experienced a much lower degree of seasonality compared to IMPROVE rural regions (Figure S.4.5b), especially in the western United States. While the seasons corresponding to maxima and minima were similar, the range in concentration between minimum and maximum months was much lower.

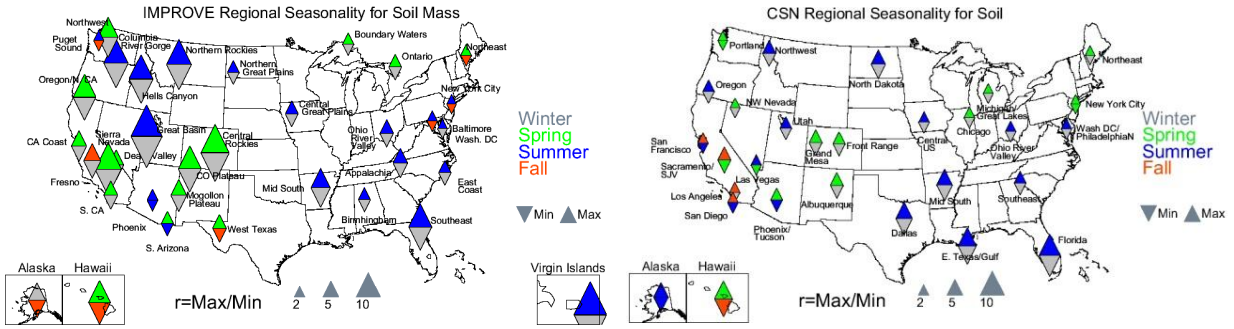

Figure S.4.5. (a) Seasonal variability for 2005–2008 monthly mean IMPROVE fine soil mass concentrations. (b) The same as (a), but for the CSN. The color of the upward-pointing triangle refers to the season with the maximum monthly mean concentration, and the downward-pointing triangle refers to the season with the minimum monthly mean concentration. The size of the triangles refers to the magnitude of the ratio of maximum to minimum monthly mean mass concentration.

S.4.6 $PM_{2.5}$ Gravimetric Fine Mass

Most of the IMPROVE regions corresponded to summer maxima and winter minima in FM monthly mean concentrations, with the exception of several regions along the eastern coast that had summer maxima and fall minima (Figure S.4.6a). Summer maxima in the western United States were most likely associated with the seasonal dominance of POM concentrations in the northwestern and southwestern United States (Figure S.4.3a). Eastern regional maxima were most likely associated with summer peaks in AS concentrations (see Figure S.4.1a). In general, FM concentrations were less seasonal compared to concentrations in individual species. Higher seasonality occurred in the western compared to the eastern United States. In contrast to the IMPROVE network, many CSN regions corresponded to winter maxima and spring minima in CSN monthly mean FM concentrations (Figure S.4.6b). The regional seasonal patterns of CSN FM concentrations were very different than the IMPROVE regional seasonal patterns. Many regions in the western United States corresponded to winter maxima and spring minima, most likely due to the prevalence of peaks in AN and POM concentrations in winter (see Figure S.4.2b). Eastern regions corresponded to summer maxima and winter and fall minima and probably were associated with summer peaks in AS concentrations, since it dominated FM in summer in this area. In general, the urban regions demonstrated a lower degree of seasonality in FM concentrations compared to rural regions.

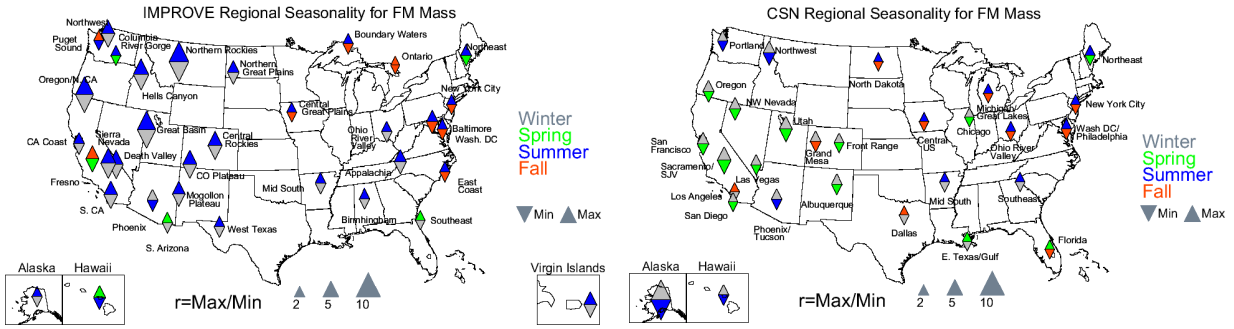

Figure S.4.6. (a) Seasonal variability for 2005–2008 monthly mean IMPROVE $PM_{2.5}$ gravimetric fine mass (FM) concentrations. (b) The same as (a), but for the CSN. The color of the upward-pointing triangle refers to the season with the maximum monthly mean concentration, and the downward-pointing triangle refers to the season with the minimum monthly mean concentration. The size of the triangles refers to the magnitude of the ratio of maximum to minimum monthly mean mass concentration.

S.4.7 Discussion

The differences observed in the seasonal and spatial patterns in species concentrations for the rural regions of the IMPROVE network and the urban locations in the CSN network are indicative of the spatial extent of aerosol sources, atmospheric processes, regional transport, and sinks. For example, AS seasonal patterns and concentrations were similar for corresponding IMPROVE rural and CSN urban regional groups, with summer maxima in the eastern half of the country. This pattern reflected the higher emissions of sulfur dioxide in this region and favorable conditions for aerosol formation in summer. Seasonal patterns in AN were consistent between CSN and IMPROVE regions. Winter maxima were observed for urban locations and in the central United States, demonstrating the regional impacts of agricultural sources in that area and favorable aerosol formation conditions during that season. CSN urban AN concentrations were considerably higher than rural IMPROVE concentrations. Maximum contributions of AN to fine mass occurred in winter for both rural and urban regions.

The strong summer maxima in POM concentrations at western rural regions contrasted with the summer/fall/winter maxima observed at CSN urban regions, suggesting that wildfire activity is a major contributor to POM concentrations in rural areas, especially in the western and northwestern United States in summer. Biogenic secondary organic aerosol also could have contributed significantly to high summer POM concentrations as well (Bench et al., 2007). Winter urban maxima at some urban regions were probably due in part to meteorological conditions but also to local sources. LAC concentrations followed patterns similar to POM concentrations, although summer maxima rural concentrations were not as dominant as POM concentrations. CSN LAC concentrations corresponding to fall/winter urban maxima were probably associated with local sources like residential heating and transportation. Both CSN POM and LAC concentrations were considerably higher than those measured in rural IMPROVE regions.

Soil concentrations were influenced by both local and long-range transport. Major regions of higher dust concentrations were evident in the urban and rural regions, especially in the southwestern United States in spring/summer and Southeast/Gulf regions in summer. Both networks had many “hot spots” of high soil that were similar in some seasons and not others,

suggesting fairly localized fugitive dust sources (Kavouras et al., 2007; 2009). The maximum contributions of soil to fine mass occurred in spring for many rural and urban regions, perhaps associated with agricultural sources. While the seasons corresponding to maxima and minima for coarse mass and fine soil concentrations agreed in some regions (e.g., the northwestern United States), for most regions these seasons did not coincide. One would expect that if soil was the main contributor to CM, their seasonality would be similar. However, based on work by Malm et al. (2007), who investigated the speciation of CM at select IMPROVE sites for a year, the speciation of CM varied significantly depending region and month. The only regions with consistent seasonal maxima and minima between soil and CM were the Columbia River Gorge, Hells Canyon, Northern Rocky Mountains, Great Basin, Death Valley, and Colorado Plateau regions. It is possible and probably quite likely that the seasonality of CM was impacted by the variability of species other than soil.

Gravimetric fine mass concentrations were noticeably higher in urban regions than rural regions. The highest concentrations of fine mass for the CSN network occurred in California, in the Sacramento/San Joaquin Valley region during December, where AN and POM composed the majority of the fine mass. Similarly, the urban IMPROVE site of Fresno had the highest fine mass concentrations in November, again dominated by AN and POM. The highest IMPROVE nonurban fine mass concentration corresponded to the Appalachia region in the eastern United States in August, where AS dominated the fine mass composition in summer.

S.5 SPATIAL AND SEASONAL PATTERNS IN RELATIVE RECONSTRUCTED AEROSOL LIGHT EXTINCTION COEFFICIENTS

Reconstructed aerosol light extinction coefficients (b_{ext}) were computed from speciated aerosol mass concentrations, multiplied by the species' extinction efficiency and the humidification factor (f(RH)), and summed over all species. The extinction algorithm used to compute b_{ext} in this report was somewhat different than the algorithm applied in previous reports, based on recommendations from a review of the algorithm (Hand and Malm, 2006). The original algorithm included contributions from $PM_{2.5}$ species such as ammonium sulfate (AS), ammonium nitrate (AN), particulate organic matter (POM), light absorbing carbon (LAC), and soil, and coarse mass (CM), and a constant term for Rayleigh scattering contributions (10 Mm^{-1}). The modified original algorithm used in this report included contributions from the above species, in addition to sea salt, site-specific Rayleigh scattering, and a change in the multiplier used to convert organic carbon to POM from 1.4 to 1.8. A similar f(RH) factor was applied to AS and AN, while an f(RH) for sea salt was computed specifically (see Chapter 3). The algorithm used in this report adopted some of the features of the revised algorithm used by the Regional Haze Rule (Pitchford et al., 2007) but applies constant mass extinction efficiency values for each aerosol component as used by the original IMPROVE algorithm. Mean light extinction coefficients computed this way should not differ significantly from those that would be obtained using the revised IMPROVE algorithm. The modified original algorithm is presented in equation S.5.1:

$$b_{ext} = 3f(RH)[\text{ ammonium sulfate}] + 3f(RH)[\text{ammonium nitrate}] + 4[\text{particulate organic matter}] + 10[\text{light absorbing carbon}] + 1[\text{soil}] + 1.7f(RH)_{ss}[\text{sea salt}] + 0.6[\text{coarse mass}] + \text{site-specific Rayleigh scattering} \quad \text{S.5.1}$$

The units of b_{ext} and Rayleigh scattering are in inverse megameters (Mm^{-1}). Mass concentrations of aerosol species are in $\mu g\ m^{-3}$, and mass scattering and absorption efficiencies have units of $m^2\ g^{-1}$. Values of 3 $m^2\ g^{-1}$ were used for both ammonium sulfate and ammonium nitrate, 4 $m^2\ g^{-1}$ for particulate organic matter, 10 $m^2\ g^{-1}$ for light absorbing carbon, 1 $m^2\ g^{-1}$ for soil, 1.7 $m^2\ g^{-1}$ for sea salt, and 0.6 $m^2\ g^{-1}$ for coarse mass. These values correspond to a wavelength of 550 nm.

Visual range and extinction measurements are nonlinear with respect to human perception of visual scene changes caused by haze. The haziness index expressed in deciview units (dv) was developed such that a 1 dv change would be a small but likely perceptible change in uniform haze conditions, regardless of the baseline visibility level (Pitchford and Malm, 1994). Haziness index values increase with increased light extinction coefficients, with a value of 0 dv corresponding to an extinction coefficient of 10 Mm^{-1}(i.e., pristine conditions). Deciview values were calculated from reconstructed total light extinction coefficients (including contributions from $PM_{2.5}$ species, coarse mass, and site-specific Rayleigh scattering instead of a constant 10 Mm^{-1}). The spatial variability in dv and b_{ext} are analogous to the spatial variability in aerosol mass concentrations; however, because of relative humidity effects on b_{ext}, the relative contributions from individual species to total b_{ext} may be different than their contributions to reconstructed fine mass.

Monthly mean (2005–2008) reconstructed b_{ext} values were computed for the major aerosol species listed earlier. These monthly mean b_{ext} values were averaged to regional means based on the IMPROVE and CSN regions discussed in section S.1 and Chapter 1. Highlights of the spatial and seasonal patterns in dv, and the seasonal and regional patterns in the monthly mean relative contribution of individual $PM_{2.5}$ species to b_{ext} are presented for AS, AN, POM, LAC, soil, and sea salt. The relative contribution of individual species to b_{ext} can vary significantly depending on the season or region and is important for understanding the causes of haze. In addition, the contribution of a given species to total b_{ext} can be quite different than its contribution to RCFM due to hygroscopic effects and relative optical efficiencies. Seasonal stacked bar charts for relative b_{ext} are grouped onto maps corresponding to four areas of the country: the northwestern, southwestern, and eastern United States, and OCONUS (Outside the Contiguous United States, e.g., Hawaii, Alaska, and Virgin Islands). Further details regarding the seasonality in absolute reconstructed b_{ext} can be found in Chapter 5, including results for CSN regions.

S.5.1 Deciview

The annual mean dv is presented in the spatial map in Figure S.5.1a. The highest dv occurred in the eastern United States and along the Ohio River valley. The values ranged from 4.65 to 22.19. The major contributor to dv in the eastern United States was AS. Higher dv values in the western United States corresponded to contributions from AN and POM. Soil contributed to dv in the southwestern United States. Further discussions of the relative contributions of individual species to visibility degradation will be provided in sections S.5.2–S.5.4.

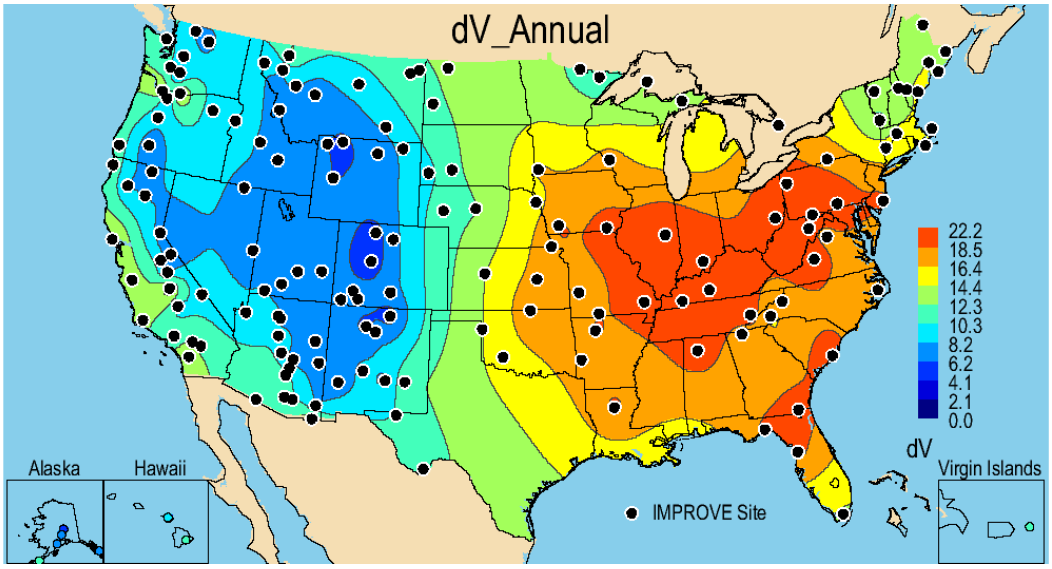

Figure S.5.1a. Annual mean $PM_{2.5}$ deciview (dv) for 2005–2008 for rural IMPROVE sites. Wavelength corresponds to 550 nm.

The seasonality in dv is shown in Figure S.5.1b. Maximum dv occurred in summer for most of the IMPROVE regions, probably associated with POM in the western and AS in the eastern United States. The high AS mass concentrations in summer in the eastern United States, along with increased relative humidity, lead to decreased visibility on regional scales during summer months. Winter maxima also occurred, as did spring. Fall maxima occurred only at the Puget Sound region. Winter and fall minima were common for most regions.

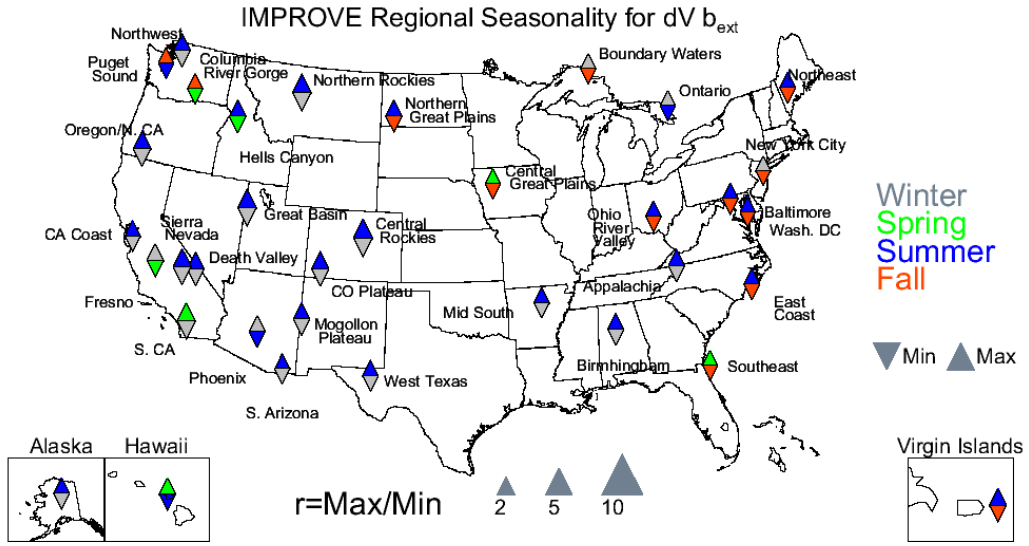

Figure S.5.1b. Seasonal variability for 2005–2008 monthly mean IMPROVE deciview (dv) light extinction coefficient (b_{ext}). The color of the upward-pointing triangle refers to the season with the maximum monthly mean concentration, and the downward-pointing triangle refers to the season with the minimum monthly mean concentration. The size of the triangles refers to the magnitude of the ratio of maximum to minimum monthly mean mass concentration.

S.5.2 Ammonium Sulfate Light Extinction Coefficients

Reconstructed light extinction coefficients from AS, b_{ext_AS}, were computed using a dry extinction efficiency of 3 m^2 g^{-1} and a humidification factor (f(RH)) to account for growth of the hygroscopic aerosol under elevated relative humidity conditions (see equation S.5.1). The b_{ext_AS} may closely resemble AS mass concentrations, but differences will arise due to hygroscopic effects. The largest relative b_{ext} contribution from AS to b_{ext} occurred at the Hawaii region in March (84.6%), most likely due to volcanic emissions, and contributions were 60% or greater year-round (Figure S.5.2.1). AS dominated b_{ext} in the eastern United States, with percent contributions ranging from 40% up to ~80% during summer (Figure S.5.2.2). The percent contribution of AS to b_{ext} was lower in the southwestern United States, roughly 20–40% at most regions (Figure S.5.2.3) but was slightly higher than the AS mass fractions in the same regions. A similar pattern was observed at the regions in the northwestern United States, where b_{ext_AS} fractions were higher than AS mass fractions. Percent contributions of AS to b_{ext} ranged from 15 to 50% and decreased during summer months at every region except the Columbia River Gorge region (Figure S.5.2.4). The seasonal b_{ext_AS} was similar to AS mass concentrations, with strong summer maxima and winter minima, However, most IMPROVE regions did not experience highly seasonal contributions of AS to b_{ext}, suggesting that AS was a consistent contributor to b_{ext} year-round.

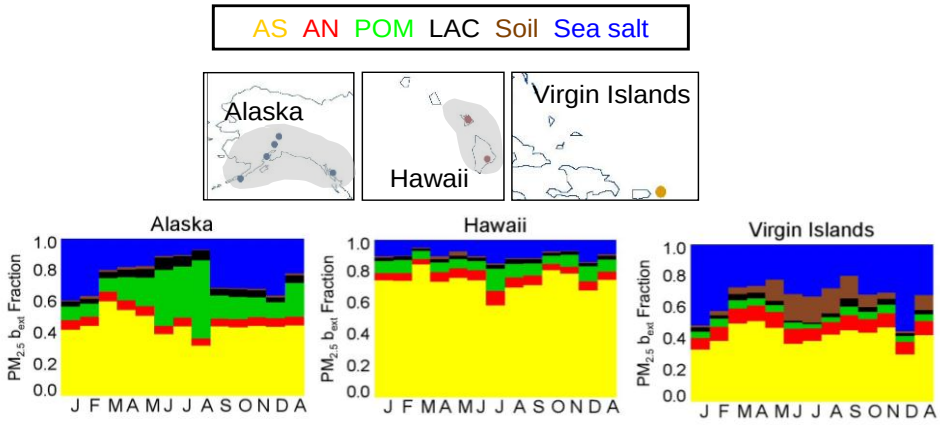

Figure S.5.2.1. IMPROVE regional monthly mean (2005–2008) $PM_{2.5}$ light extinction coefficient (b_{ext}) fractions for Hawaii, Alaska, and the Virgin Islands. The letters on the x-axis correspond to the month and "A" corresponds to "annual" mean. Ammonium sulfate (AS) is in yellow, ammonium nitrate (AN) in red, particulate organic matter (POM) in green, light absorbing carbon (LAC) in black, soil in brown, and sea salt in blue. The shaded area corresponds to the regions that comprise the sites, shown as dots.

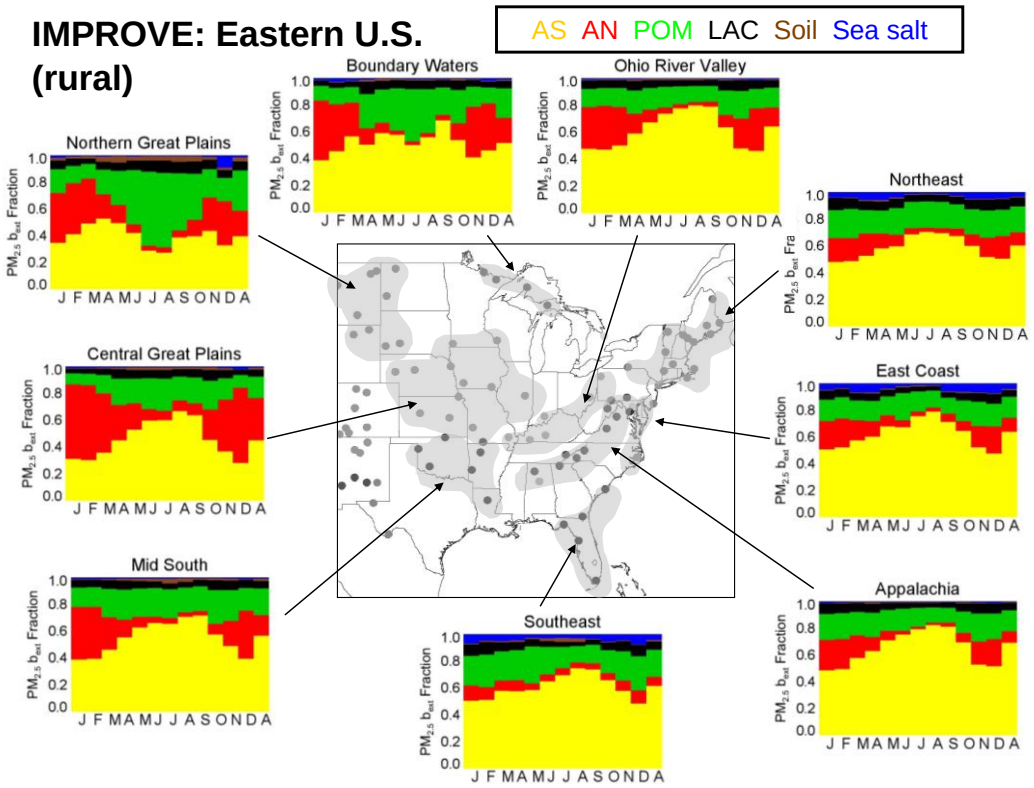

Figure S.5.2.2. IMPROVE regional monthly mean (2005–2008) $PM_{2.5}$ light extinction coefficient (b_{ext}) fractions for the eastern United States. The letters on the x-axis correspond to the month and "A" corresponds to "annual" mean. Ammonium sulfate (AS) is in yellow, ammonium nitrate (AN) in red, particulate organic matter (POM) in green, light absorbing carbon (LAC) in black, soil in brown, and sea salt in blue. The shaded area corresponds to the regions that comprise the sites, shown as dots.

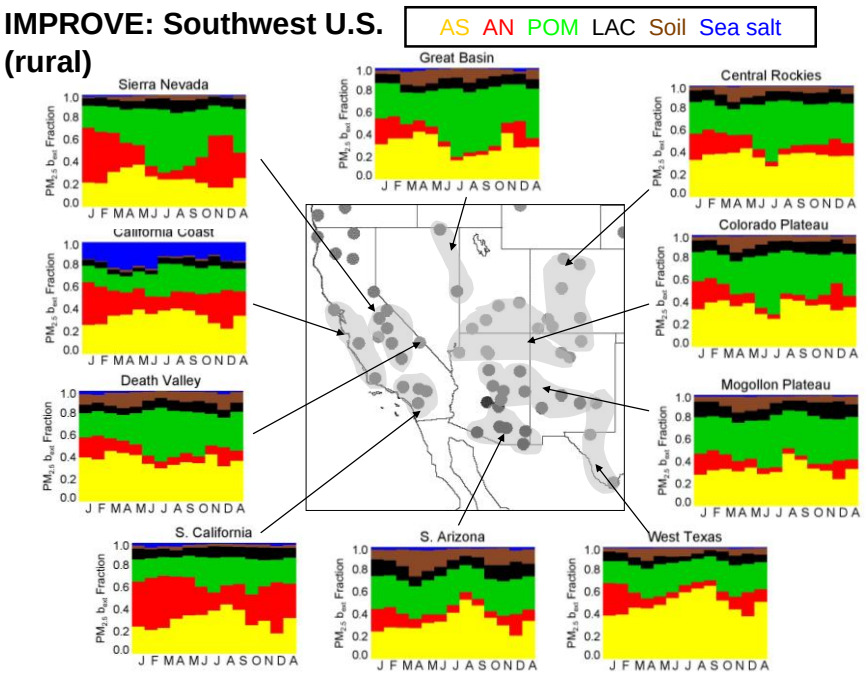

Figure S.5.2.3. IMPROVE regional monthly mean (2005–2008) $PM_{2.5}$ light extinction coefficient (b_{ext}) fractions for the southwestern United States. The letters on the x-axis correspond to the month and "A" corresponds to "annual" mean. Ammonium sulfate (AS) is in yellow, ammonium nitrate (AN) in red, particulate organic matter (POM) in green, light absorbing carbon (LAC) in black, soil in brown, and sea salt in blue. The shaded area corresponds to the regions that comprise the sites, shown as dots.

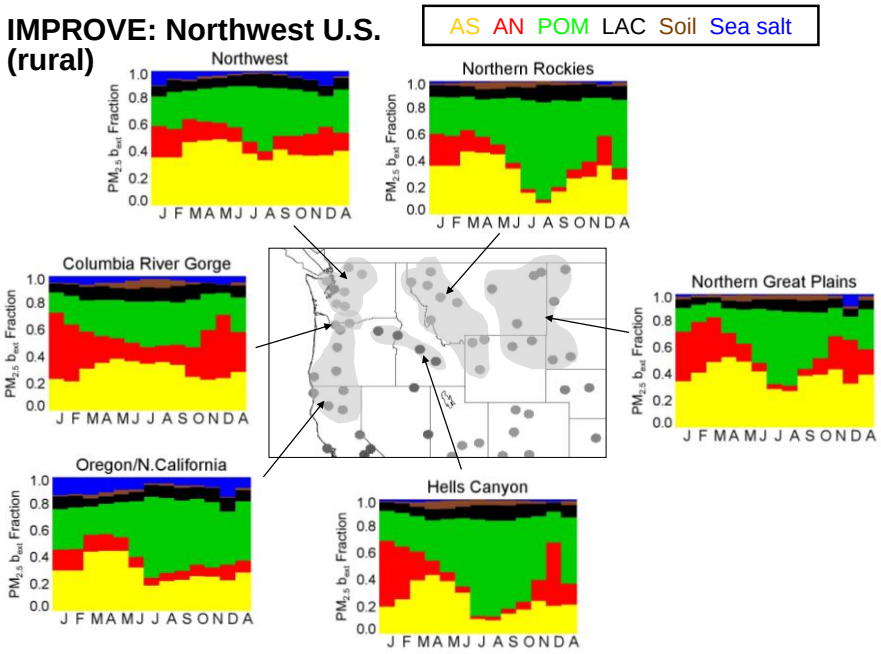

Figure S.5.2.4. IMPROVE regional monthly mean (2005–2008) $PM_{2.5}$ light extinction coefficient (b_{ext}) fractions for the northwestern United States. The letters on the x-axis correspond to the month and "A" corresponds to "annual" mean. Ammonium sulfate (AS) is in yellow, ammonium nitrate (AN) in red, particulate organic matter (POM) in green, light absorbing carbon (LAC) in black, soil in brown, and sea salt in blue. The shaded area corresponds to the regions that comprise the sites, shown as dots.

S.5.3 Ammonium Nitrate Light Extinction Coefficients

The extinction efficiency and f(RH) values used to compute the contributions of AN to b_{ext} (b_{ext_AN}) were the same as those used to compute b_{ext_AS}. In a similar manner, while general spatial and seasonal patterns of b_{ext_AN} mostly follow AN mass concentrations, differences may occur due to hygroscopic effects. The AN contributions to b_{ext} were generally the lowest in the eastern United States (Figure S.5.2.2). Values reached 40% or more in winter at regions in the central United States. In fact, AN dominated the IMPROVE b_{ext} in the Central Great Plains region in December (56.2%) (Figure S.5.2.2). Contributions of AN to b_{ext} were even higher than its contributions to reconstructed fine mass (RCFM) at these regions, in part due to its hygroscopic properties and higher extinction efficiencies relative to other species (e.g., soil). Percent contributions of AN to b_{ext} of 40% were common at rural IMPROVE regions in the northwestern United States (Figure S.5.2.4). The relative contribution of AN to b_{ext} was somewhat lower in the southwestern United States (Figure S.5.2.3). Values near 20% were more common for regions in this area, although higher contributions in the winter still occurred. These regions also experienced higher contributions of AN to b_{ext} compared to RCFM but not to the same degree as other regions in the United States. Compared to other regions, the AN contributions to b_{ext} in the OCONUS regions were relatively low (<10%) (Figure S.5.2.1). Most IMPROVE regions showed a high degree of seasonality for the contribution of AN to b_{ext}, and most regions corresponded to winter maxima and summer minima.

S.5.4 Particulate Organic Matter Light Extinction Coefficients

POM light extinction coefficients (b_{ext_POM}) were scaled to POM mass because, unlike AS and AN, POM was considered nonhygroscopic. On a similar dry mass basis, b_{ext_POM} would be higher than that for b_{ext_AS} or b_{ext_AN}, because its extinction efficiency was higher (4 m^2 g^{-1} versus 3 $m^2 g^{-1}$). While the patterns of b_{ext_POM} were the same as those of POM mass concentrations, its relative contribution to reconstructed b_{ext} was not because of the hygroscopic and optical properties of other species contributing to b_{ext}. In the eastern United States, the b_{ext_POM} fraction was generally lower than the POM mass fraction at several regions, due to the increased importance of hygroscopic AS on b_{ext}. The percent contribution of POM to b_{ext} was fairly constant year-round at most regions in the eastern United States (Figure S.5.2.2). Contributions of POM to b_{ext} were significant at regions in the northwestern United States (Figure S.5.2.4); however, the relative b_{ext_POM} values were generally lower than POM mass fraction for these regions. POM contributions to b_{ext} were typically 20–30% at most regions in the southwestern United States (Figure S.5.2.3). The Alaska region was the only OCONUS region that had considerable contributions of POM to b_{ext} (Figure S.5.2.1). These contributions peaked in summer and dropped off fairly rapidly in fall, probably related to biomass burning emissions. Relative contributions of POM to b_{ext} were fairly low (~10% or less) in the Hawaii and Virgin Islands regions. The relative b_{ext_POM} had a much lower degree of seasonality compared to absolute b_{ext_POM}, especially in the western United States. Summer maxima were still the most common.

S.5.5 Light Absorbing Carbon Light Extinction Coefficients

Light extinction coefficients due to LAC (b_{ext_LAC}) were computed by scaling the LAC mass by its extinction efficiency (10 m^2 g^{-1}), which is higher than the other species due to its

ability to both scatter and absorb visible light. This higher extinction efficiency increased LAC's relative contribution to b_{ext} compared to its contributions to RCFM, especially at most regions in the eastern United States. Contributions were less than 10% at most regions and higher in fall and winter (Figure S.5.2.2). Somewhat higher LAC contributions to b_{ext} occurred for regions in the southwestern United States (Figure S.5.2.3). Relative b_{ext_LAC} contributions of 10% or more were common at most regions in the northwestern United States and fairly steady year-round (Figure S.5.2.4). Of the OCONUS regions, the Alaska region had the highest b_{ext_LAC} contributions (Figure S.5.2.1). The Hawaii and Virgin Islands regions had the lowest b_{ext_LAC} contributions of any regions in the United States; in fact, the smallest contribution in the United States occurred at the Virgin Islands region in July (0.97%). The relative b_{ext_LAC} had a much lower degree of seasonality compared to absolute b_{ext_LAC}, especially in the western United States. Summer minima were common in the eastern United States and at some regions in the southwestern United States.

S.5.6 $PM_{2.5}$ Soil Mass Light Extinction Coefficients

The soil extinction efficiency used to compute light extinction coefficients from soil (b_{ext_soil}) was 1 m^2g^{-1}. Soil is nonhygroscopic, therefore b_{ext_soil} values were the same as the soil mass concentrations, as were its seasonal and regional patterns. Relative contributions of soil to b_{ext} in the eastern United States were negligible at most rural regions, reaching only a few percent (Figure S.5.2.2). In contrast, soil contributions to RCFM reached 10–20% at these same regions, depending on time of year. Compared to the eastern United States, soil contributions to b_{ext} were higher in the southwestern United States and reached up to 15–20%, especially during spring months (Figure S.5.2.3). However, at these same regions soil contributed up to 50% to RCFM. Contributions of only a few percent were common at regions in the northwestern United States Figure S.5.2.4). Soil contributions to b_{ext} reached ~20% at the Virgin Islands region during summer (Figure S.5.2.1); however its contribution to RCFM was near 60% during the same months. Relative b_{ext_soil} values were low at other OCONUS regions. Strong seasonality in relative b_{ext_soil} for IMPROVE regions was observed. Contributions to b_{ext} from soil were typically highest in the spring. Most regional minima occurred during winter for relative b_{ext_soil}.

S.6 TRENDS IN IMPROVE SPECIATED AEROSOL MASS CONCENTRATIONS

As stated in the IMPROVE objectives, one of the main purposes of the network is to document long-term trends for assessing progress towards the national visibility goals. Twenty years of data were available to evaluate trends in this report for many sites within the IMPROVE network. Trend analyses were performed for "long-term" (1989–2008) and "short-term" (2000–2008) time periods for eight parameters: annual mean, 10^{th}, 50^{th}, and 90^{th} percentiles, and four seasons (winter, spring, summer, and fall). A Theil regression was performed with the concentration data as the dependent variable and the year as the independent variable (Theil, 1950). A trend was considered statistically significant at 5% ($p \leq 0.05$), meaning that there was a 95% chance that the slope was not due to random chance. Trends that were significant at 15% ($0.05 < p \leq 0.15$) are also reported. Further details regarding the linear regression calculations are provided in Chapter 6. "Trend" is defined as percent change per year (% yr^{-1}) and was computed by dividing the slope derived from the Theil regression by the median mass concentration value over the time period of the trend at a given site, multiplied by 100%. Reporting trend instead of

slope reflects the relative change in concentration at a given site. However, trends can be quite large (>100%) when median concentrations are very low (e.g., 10th percentile).

Long-term trends for sulfate ion, total carbon (TC = organic carbon + light absorbing carbon), fine soil, fine mass (FM), coarse mass (CM), and PM_{10} concentrations were computed. In addition to the species listed above, short-term trends were computed for nitrate ion. Highlights from the trend analyses are presented here; details can be found in Chapter 6.

Trend results for each species and site are presented on maps of the United States. Sites with positive trends with significance levels of 95% and greater ($p \leq 0.05$) correspond to solid red, upward-pointing triangles. Positive trends with significance levels of 85–95% ($0.05 < p \leq 0.15$) correspond to red, unfilled, upward-pointing triangles. A similar methodology was applied to sites with decreasing trends but in blue. Sites with insignificant trends correspond to black-filled triangles. The size of the triangle corresponds to the magnitude of the trend, with the same scale maintained for all species and parameters for comparison purposes. Sites with no significant trends are shown as black triangles.

S.6.1 Sulfate Ion Trends

Decreasing trends in sulfate ion concentrations were typical for most IMPROVE sites, regardless of the percentile, season, or time period. Both the 10th percentile and winter season corresponded to sites with large negative significant trends as shown in the map of average winter long-term sulfate ion trends in Figure S.6.1.1. Recall that the lowest concentrations in regional mean ammonium sulfate (derived from sulfate ion concentrations) from 2005 through 2008 occurred during winter in the southwestern United States (see Figure S.4.1a). The long-term trends suggested that the lowest sulfate ion concentration days, most likely occurring in winter, have been decreasing for several years at many sites.

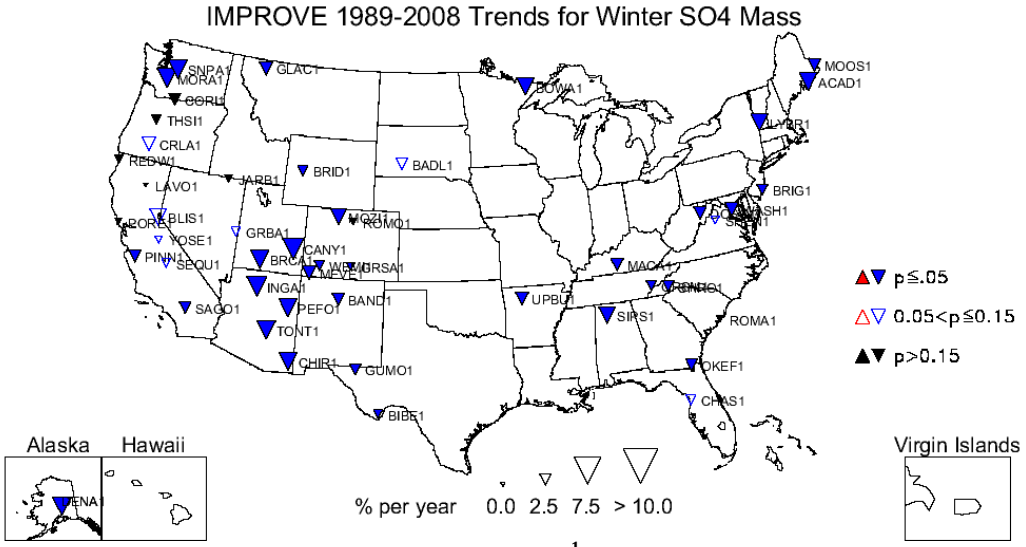

Figure S.6.1.1. Long-term (1989–2008) trends (% yr^{-1}) in average winter sulfate ion mass concentrations. Sites with statistically significant trends ($p \leq 0.05$) are designated by filled red (increasing) and blue (decreasing) triangles. Insignificant trends ($p > 0.15$) are designated by filled black triangles.

In comparison, the 90th percentile, spring and summer season trends in sulfate ion concentrations were less negative (not shown). In fact, positive long-term trends occurred at Big Bend, Texas (BIBE1), for the 90th percentile and spring season and also at Lassen Volcanic NP, California (LAVO1), during summer. These sites were the only IMPROVE locations that corresponded to positive sulfate ion trends for any long-term trend parameter investigated.

A larger number of sites had significant positive short-term sulfate ion trends compared to the long-term trends. In fact, some sites with decreasing long-term trends had positive short-term trends. For example, sulfate ion concentrations at the Denali, Alaska, site (DENA1) started increasing in later years. Upward-trending sulfate ion concentrations occurred during the most recent 10 years at DENA1, which was the period evaluated for the short-term trend analyses.

The least negative overall short-term sulfate ion trends occurred for the 50th percentile and spring season. Short-term sulfate ion trends during spring were very interesting, as shown in Figure S.6.1.2. Many sites in the western United States corresponded to positive trends in the spring, the only season to exhibit such patterns. Recall that the maximum monthly mean ammonium sulfate concentrations also occurred in spring for many regions in the western United States (see Section S.4.1).

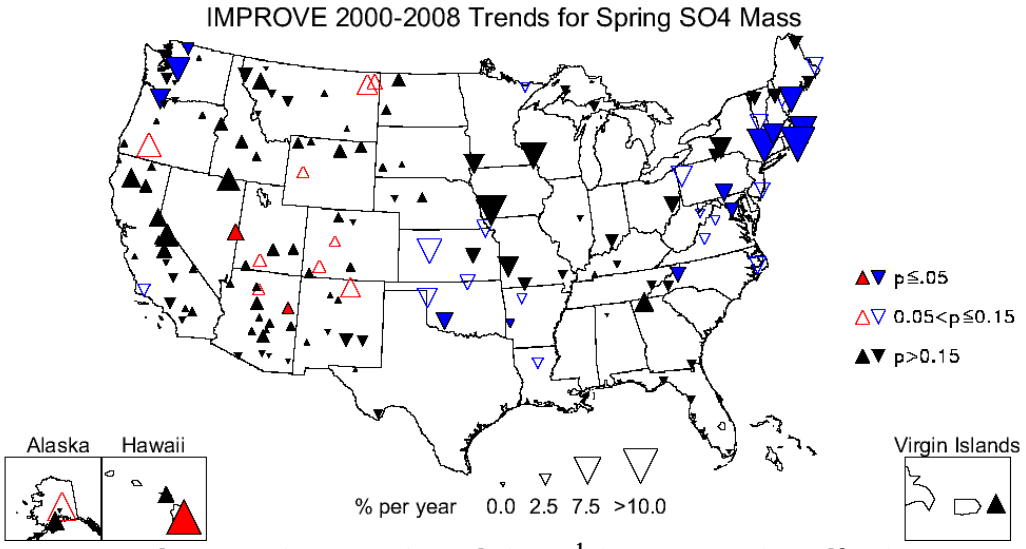

Figure S.6.1.2. Short-term (2000–2008) trends (% yr^{-1}) in average spring sulfate ion mass concentrations. Sites with statistically significant trends (p≤0.05) are designated by filled red (increasing) and blue (decreasing) triangles. Insignificant trends (p>0.15) are designated by filled black triangles.

S.6.2 Nitrate Ion Trends

During the late 1990s, IMPROVE nitrate ion concentrations at many sites fell below historical values during winter months. Investigations into a period from 1996 to 2000 revealed lower than usual concentrations during winter months, and the cause remains unknown (McDade, 2007). Concentrations returned to normal levels after 2000, after which the data were deemed valid. Given these uncertainties in earlier nitrate ion concentrations, only short-term trends for nitrate ion concentrations were computed.

The 10th percentile nitrate ion trends at most sites were relatively large compared to the sulfate ion trends and highly significant ($p<0.05$) at most sites around the United States (see Figure S.6.2.1). No sites were associated with positive 10th percentile, short-term nitrate ion trends. Large decreasing trends occurred for sites all around the United States during fall months, and no positive trends occurred at any site for fall or summer seasons.

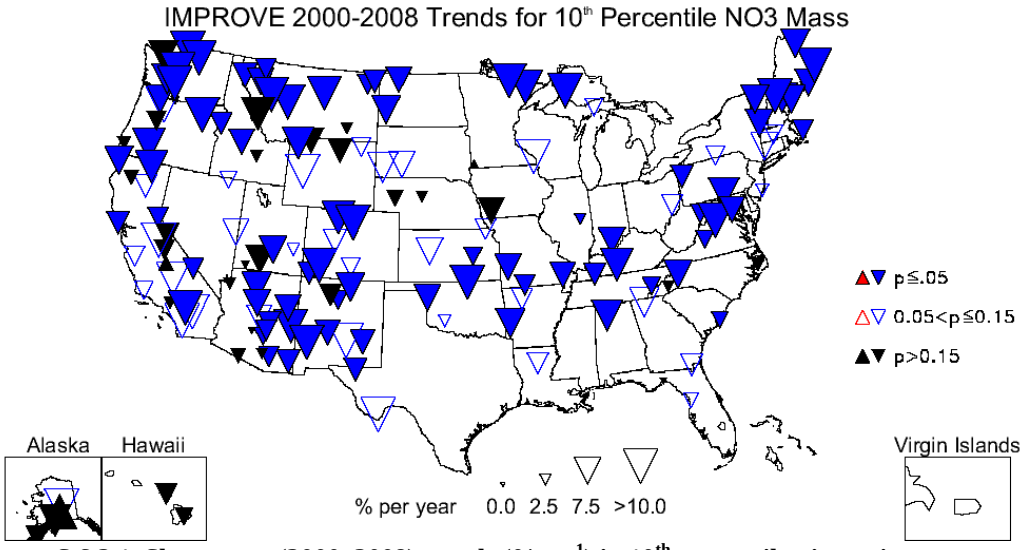

Figure S.6.2.1. Short-term (2000–2008) trends (% yr^{-1}) in 10th percentile nitrate ion mass concentrations. Sites with statistically significant trends ($p\leq0.05$) are designated by filled red (increasing) and blue (decreasing) triangles. Insignificant trends ($p>0.15$) are designated by filled black triangles.

A map for the 50th percentile trends is shown in Figure S.6.2.2. As was the case with the trends for the 10th percentile and fall season, the magnitude of 50th percentile nitrate ion trends was fairly consistent for most sites across the United States, although several sites in the Mountain West corresponded to less significant ($p\leq0.15$) negative trends. Positive trends occurred at several sites, including the Virgin Islands (VIIS1) and Denali, Alaska (DENA1), where the maximum monthly mean ammonium nitrate concentrations also occurred during spring months.

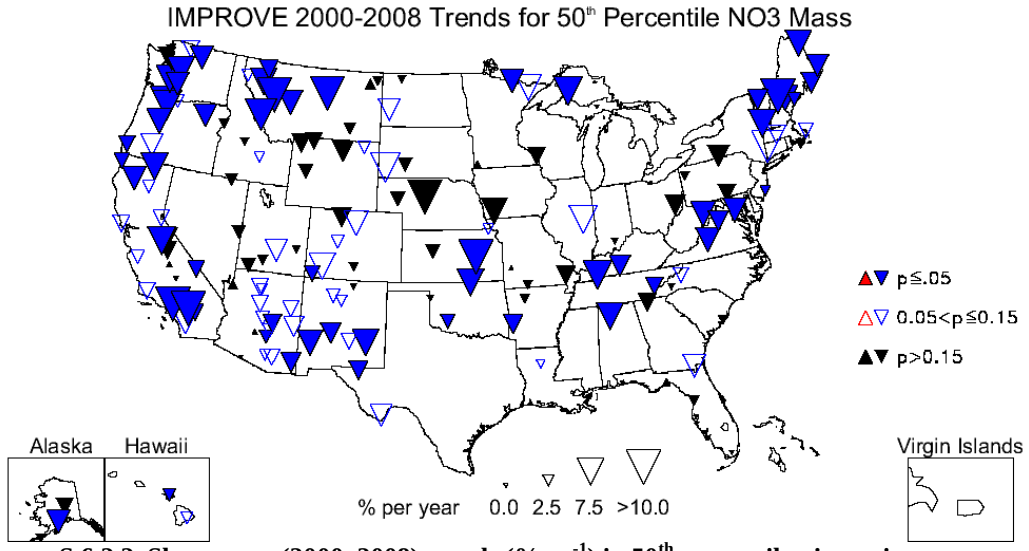

Figure S.6.2.2. Short-term (2000–2008) trends (% yr^{-1}) in 50th percentile nitrate ion mass concentrations. Sites with statistically significant trends (p≤0.05) are designated by filled red (increasing) and blue (decreasing) triangles. Insignificant trends (p>0.15) are designated by filled black triangles.

S.6.3 Total Carbon Trends

Trends in TC, rather than on OC and LAC, were computed because changes in analytical methods due to hardware upgrades on January 1, 2005, resulted in potential changes in the split between OC and LAC that introduced uncertainty to trend analyses (Chow et al., 2007; White, 2007). Higher LAC/TC ratios were reported after the change in analytical methods, but no changes in total carbon were detected.

The largest negative long-term TC trends corresponded to the 10th percentile and winter season (see map of 10th percentile TC trends in Figure S.6.3.1). Sites with larger negative trends were located along the western coast. No positive trends were associated with any site for 10th percentile concentrations. The winter season was also associated with large decreasing trends and corresponded to sites in the western United States. It is possible that the low TC concentrations associated with the 10th percentile occurred mainly in winter; in the western United States both OC and LAC were associated with minimum monthly mean concentrations (2005–2008) during winter months for many regions (see Figure S.4.3.a and Figure S.4.4.b, respectively). Concentrations on these already low concentration days in winter appeared to be decreasing.

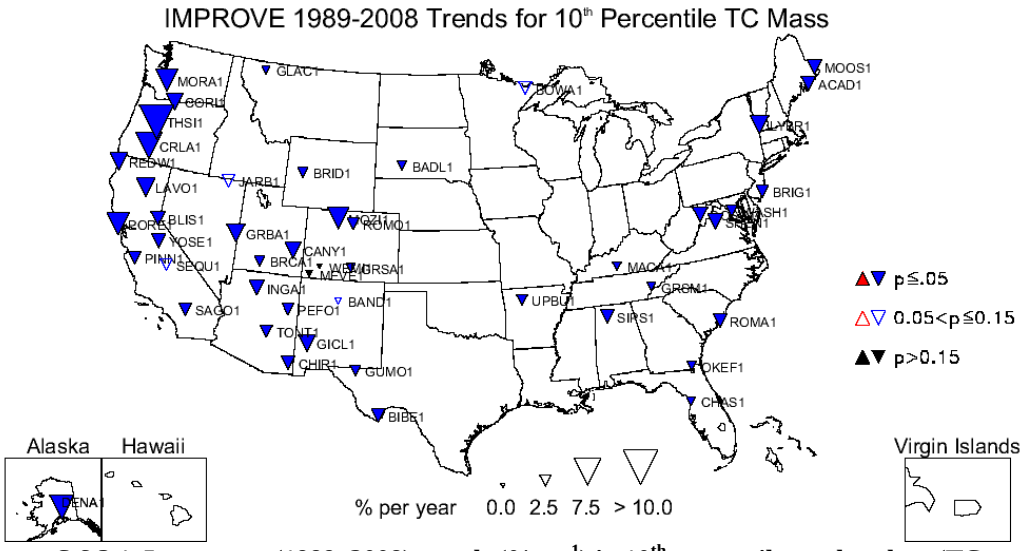

Figure S.6.3.1. Long-term (1989–2008) trends (% yr^{-1}) in 10th percentile total carbon (TC = organic carbon + light absorbing carbon) mass concentrations. Sites with statistically significant trends (p≤0.05) are designated by filled red (increasing) and blue (decreasing) triangles. Insignificant trends (p>0.15) are designated by filled black triangles.

Long-term, summer TC trends were associated with the largest number of significant positive trends of all parameters. Magnitudes of summer trends were fairly consistent (and low) around the United States. Recall that most regions in the western United States corresponded to summer maxima in both OC and LAC concentrations (Figures S.4.3.b and S.4.4.b, respectively). Unlike the strongly decreasing TC 10th percentile concentrations that likely occurred during winter days, the highest concentrations that were likely associated with summer months were decreasing to a much lower degree and at some sites actually increasing.

Short-term TC trends were much larger for many sites around the United States compared to long-term trends. There were no sites associated with positive short-term TC trends for any of the percentiles. Spring, summer, and fall, short-term, TC trends were associated with positive trends, with summer having the highest number.

S.6.4 Gravimetric $PM_{2.5}$ Fine Mass Trends

Given the previous discussions, one might attempt to deduce trends in $PM_{2.5}$ fine mass (FM), as it is largely composed of the species presented in previous sections. However, inferring FM trends based on the trends of other species is complicated because of the difference in the behavior and seasonality of a given species in relation to another. Due to sampling artifacts like those discussed in Chapter 8, FM does not equal the simple sum of all species. Finally, the significance level of trends at a given site may differ for individual species and for FM, complicating comparisons of trends at a specific location.

The magnitudes of 10th percentile, long-term FM trends were fairly similar across the United States, although sites in the southeastern United States had less negative trends, similar to the sulfate ion and TC 10th percentile trends (Figure S.6.4.1). No sites were associated with positive 10th percentile trends. Winter long-term FM trends were larger in magnitude (more

negative) at most sites compared to 10th percentile trends, and no sites corresponded to positive winter trends. FM monthly mean concentrations (2005–2008) were at a minimum during winter months for many regions in the United States (Figure S.4.6b). The negative winter trends suggested that the days with the lowest FM concentrations were getting cleaner.

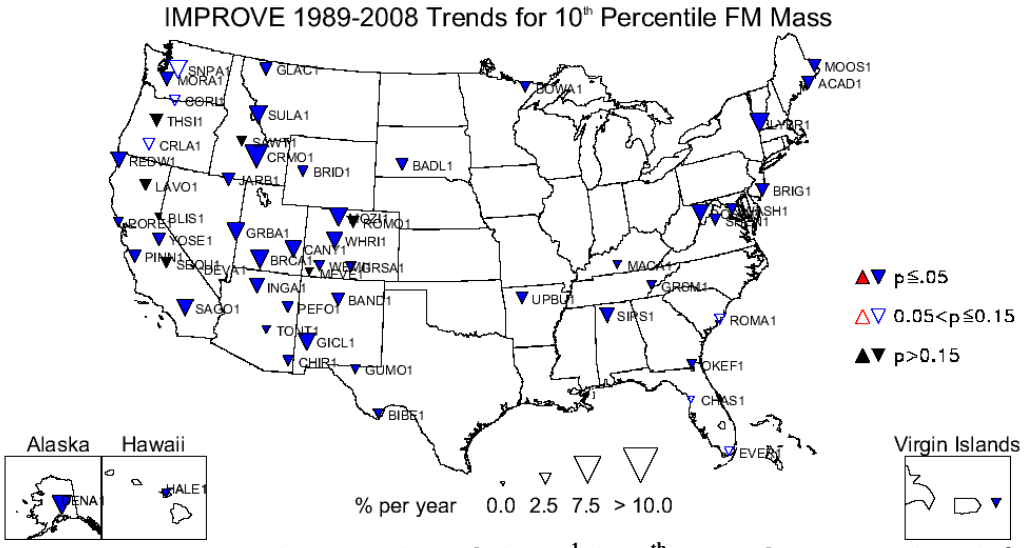

Figure S.6.4.1. Long-term (1989–2008) trends (% yr^{-1}) in 10th percentile $PM_{2.5}$ gravimetric fine mass (FM) concentrations. Sites with statistically significant trends (p≤0.05) are designated by filled red (increasing) and blue (decreasing) triangles. Insignificant trends (p>0.15) are designated by filled black triangles.

Positive long-term FM trends were associated with the 90th percentile and spring, summer, and fall seasons. Long-term FM trends in the summer in the eastern United States were decreasing at most sites. Many sites in the western United States were associated with either low, negative long-term FM trends or trends that were statistically insignificant. Most of the regions in the United States were associated with maximum FM monthly mean concentrations in the summer months (see Figure S.4.6.1b). Trend results suggested that these summer FM concentrations appeared to be decreasing less over time compared to other seasons.

All of the short-term FM trend parameters included some sites with positive trends. Several sites had positive 50th percentile, short-term trends, and eleven sites were associated with positive trends in fall, more than any other season. Most of these sites were located in the western United States and in Alaska and Hawaii. No sites in the eastern United States were associated with positive fall trends. The only species to be associated with positive short-term fall trends in the western United States were the sulfate ion (in Alaska, Hawaii and Arizona), soil (several sites in the western United States.), and total carbon at a couple of western sites; therefore the fall positive trends in FM in the western United States could be driven by different species, depending on the site.

Additional discussions of IMPROVE trends, including results for soil, CM, and PM_{10} can be found in Chapter 6. No trends were computed for CSN data because trends are sensitive to changes in CSN sampling methodology (e.g., sampler and analytical methodology vary from site to site and over time) and the network's shorter duration (established in 2000 with additional sites coming online over a period of several years).

The trend results presented in this section were intended as a summary of the temporal changes in the mass concentrations of major aerosol species over short and long time periods. Results suggested that, for most species, concentrations were decreasing at IMPROVE sites around the United States, and these decreasing trends were largest for the lowest concentrations and during winter seasons. Because normalized trends were presented, it is not surprising that the 10^{th} percentile trends were typically the largest in magnitude because they were normalized with the lowest concentrations. This general result may not hold for individual sites or for given species (e.g., soil) but overall this consistent pattern emerged. A similar pattern was reported in *Air Quality in National Parks 2009 Annual Performance and Progress Report* (NPS, 2010), which demonstrated larger decreasing trends in deciview on the clearest days compared to the haziest days.

S.7 REGIONAL HAZE RULE METRICS

The EPA established the Regional Haze Rule in 1999 (RHR, U.S. EPA, 1999), a major effort to improve air quality in national parks and wilderness areas. The RHR calls for state and federal agencies to collaborate to improve visibility in 156 visibility-protected federal Class I areas (CIA) (see Figure 1.1 in Chapter 1). The RHR specifies a default method to track progress towards the national visibility goal of no anthropogenic visibility impairment. The RHR focuses on reducing pollution on the 20% worst visibility days each year while allowing no degradation of the 20% best visibility days. Haziness is defined by the deciview metric and is calculated using the "original" IMPROVE algorithm (RHR1) or the "revised" IMPROVE algorithm (RHR2) (Pitchford et al., 2007). Since nearly all states and regional planning organizations used the RHR2 algorithm for state implementation plan development, modeling, and source apportionment, the RHR2 algorithm was applied in the analyses presented in Chapter 9. The RHR2 algorithm differs from that applied in the rest of the report in that it applies size mode-dependent mass extinction efficiencies.

Central to the RHR is the concept of the uniform rate of progress (URP). The URP is the yearly rate of change required to achieve natural dv conditions by 2064 in a linear fashion beginning in 2004. The URP provides a reference to evaluate progress made in the context of the change required to reach natural conditions in 60 years. It should be noted that the nature of emissions control programs makes it likely that actual progress will be somewhat erratic and that failure to achieve the URP at any point in the process should be considered in the context of changes to emissions inventories.

Descriptions and evaluations of RHR metrics are provided in Chapter 9 and Appendix G and H. These evaluations focus on comparisons of the 20% worst and best visibility days for the baseline (2000–2004) and period 1 (2005–2009) time periods. Summaries of the changes from baseline to period 1 compared to the URP are presented on maps to evaluate regional progress toward natural conditions. Detailed timelines and yearly data are also presented for case studies in Chapter 9 and for all complete IMPROVE regional haze tracking sites, organized by state, in Appendix H. The analysis provided in Chapter 9 is intended as an evaluation of the progress towards meeting RHR goals and should not necessarily be interpreted in the context of regulatory requirements.

REFERENCES

Bench, G., S. Fallon, B. Schichtel, W. Malm, and C. McDade (2007), Relative contributions of fossil and contemporary carbon sources to PM2.5 aerosols at nine Interagency Monitoring of Protected Visual Environments (IMPROVE) network sites, *J. Geophys. Res., 112,* D10205, doi:10.1029/2006JD007708.

Bond, T. C., and R. W. Bergstrom (2006), Light absorption by carbonaceous particles: An investigative review, *Aerosol Sci. Techno., 40,* 27-67.

Chow, J. C., J. G. Watson, L. C. Pritchett, W. R. Pierson, C. A. Frazier, and R. G. Purcell (1993), The DRI thermal/optical reflectance carbon analysis system: Description, evaluation and applications in U.S. air quality studies, *Atmos. Env., 27A(8),* 1185-1201.

Chow, J. C., J. G. Watson, L.-W. A. Chen, M. C. O. Chang, N. F. Robinson, D. Trimble, and S. Kohl (2007), The IMPROVE_A temperature protocol for thermal/optical carbon analysis: Maintaining consistency with a long-term database, *J. Air & Waste Manage. Assoc., 57,* 1014-1023.

Debell, L. J., K. Gebhart, J. L. Hand, W. C. Malm, M. L. Pitchford, B. A. Schichtel, and W. H. White (2006), IMPROVE (Interagency Monitoring of Protected Visual Environments): Spatial and seasonal patterns and temporal variability of haze and its constituents in the United States: Report IV, CIRA Report ISSN: 0737-5352-74, Colo. State Univ., Fort Collins, http://vista.cira.colostate.edu/improve/Publications/Reports/2006/2006.htm.

Hand, J. L., and W. C. Malm (2006), Review of the IMPROVE equation for estimating ambient light extinction coefficients, CIRA Report, ISSN: 0737-5352-71, Colo. State Univ., Fort Collins.

Kavouras, I. G., V. Etyemezian, J. Xu, D. W. Dubois, M. Green, and M. Pitchford (2007), Assessment of the local windblown component of dust in the western United States, *J. Geophys. Res., 112,* D08211, doi:10.1029/2006JD007832.

Kavouras, I. G., V. Etyemezian, D. W. Dubois, J. Xu, and M. Pitchford (2009), Source reconciliation of atmospheric dust causing visibility impairment in Class I areas of the western United States, *J. Geophys. Res., 114,* D02308, doi:10.1029/2008JD009923.

Malm, W. C., J. F. Sisler, M. L. Pitchford, M. Scruggs, R. Ames, S. Copeland, K. A. Gebhart, and D. E. Day (2000), IMPROVE (Interagency Monitoring of Protected Visual Environments): Spatial and seasonal patterns and temporal variability of haze and its constituents in the United States: Report III, CIRA Report ISSN: 0737-5352-47, Colo. State Univ., Fort Collins, http://vista.cira.colostate.edu/improve/Publications/Reports/2000/2000.htm.

Malm, W. C., M. L. Pitchford, C. McDade, and L. L. Ashbaugh (2007), Coarse particle speciation at selected locations in the rural continental United States, *Atmos. Environ., 41,* 2225-2239.

Malm, W. C., B. A. Schichtel, and M. L. Pitchford (2011), Uncertainties in $PM_{2.5}$ gravimetric and speciation measurements and what we can learn from them, *J. Air Waste Manage,* In press.

McDade, C. E. (2007), Diminshed wintertime nitrate concentrations in the late 1990s, Doc. # da0002, http://vista.cira.colostate.edu/improve/Data/QA_QC/Advisory/da0002/da0002_WinterNO3.pdf).

NPS (2010), Air quality in National Parks, 2009 Annual Performance and Progress Report, Natural Resource Report NPS/NRPC/ARD/NRR-2010/266., http://www.nature.nps.gov/air/Pubs/pdf/gpra/AQ_Trends_In_Parks_2009_Final_Web.pdf

Pitchford, M., W. Malm, B. Schichtel, N. Kumar, D. Lowenthal and J. Hand (2007), Revised algorithm for estimating light extinction from IMPROVE particle speciation data, *J. Air & Waste Manage. Assoc., 57,* 1326-1336.

Pitchford, M. L. and W. C. Malm (1994), Development and applications of a standard visual index, *Atmos. Environ, 28,* 5, 1049-1054.

Sisler, J. F., D. Huffman, and D. A. Latimer (1993), Spatial and temporal patterns and the chemical composition of the haze in the United States: An analysis of data from the IMPROVE network, 1988–1991, CIRA Report ISSN: 0737-5352-26, Colo. State Univ., Fort Collins, http://vista.cira.colostate.edu/improve/Publications/Reports/1993/1993.htm.

Sisler, J. F., W. C. Malm and K. G. Gebhart (1996), Spatial and seasonal patterns and long term variability of the composition of haze in the United States: An analysis of data from the IMPROVE network, CIRA Report ISSN: 0737-5352-32, Colo. State Univ., Fort Collins, http://vista.cira.colostate.edu/improve/Publications/Reports/1996/1996.htm.

Tanner, R. L., W. J. Parkhurst, M. L. Valente, and W. D. Phillips (2004), Regional composition of $PM_{2.5}$ aerosols measured at urban, rural, and "background" sites in the Tennessee valley, *Atmos. Environ., 38,* 3143-3153.

Theil, H. (1950), A rank-invariant method of linear and polynomial regression analysis, *Proc. Kon. Ned. Akad. V. Wetensch. A., 53,* 386-392, 521-525, 1397-1412.

Turpin, B. J., and H.-J. Lim (2001), Species contributions to $PM_{2.5}$ mass concentrations: Revisiting common assumptions for estimating organic mass, *Aerosol Sci. Technol., 35,* 602-610.

U.S. EPA (1999), Regional Haze Regulations; Final Rule, 40 CFR 51, Federal Register, 64, 35714-35774.

White, W. H. (2007), Shift in EC/OC split with 1 January 2005 TOR hardware upgrade, Doc. # da0016, http://vista.cira.colostate.edu/improve/Data/QA_QC/Advisory/da0016/da0016_TOR2005.pdf.